Interferon-α 2b–induced thrombocytopenia is caused by inhibition of platelet production but not proliferation and endomitosis in human megakaryocytes

*Akiko Yamane,[1] *Takanori Nakamura,[1,2] Hidenori Suzuki,[3] Mamoru Ito,[4] Yasuyuki Ohnishi,[4] Yasuo Ikeda,[1] and Yoshitaka Miyakawa[1]

[1]Division of Hematology, Department of Internal Medicine, Keio University School of Medicine, Tokyo; [2]Biological Research Laboratories, Nissan Chemical Industries, Saitama; [3]Medical Research and Development Center, Tokyo Metropolitan Institute of Medical Science, Tokyo; and [4]Central Institute for Experimental Animals, Kanagawa, Japan

Human interferon (IFN)- is the standard therapy for chronic hepatitis C to prevent its progression to liver cirrhosis and hepatocellular carcinoma. Thrombocytopenia is one of the major adverse effects of IFN- and often leads to dose reduction or treatment discontinuation. However, there is little information on how IFN- inhibits human megakaryopoiesis. In this study, we demonstrated that IFN- did not inhibit colony formation of megakaryocytes from human CD34 hematopoietic stem cells. IFN- did not inhibit endomitosis but did inhibit cytoplasmic maturation of megakaryocytes and platelet production in vitro. IFN- suppressed the expression of transcription factors regulating late-stage megakaryopoiesis, such as GATA-1, p45$^{NF\text{-}E2}$, and MafG. IFN- also significantly reduced the number of human platelets but not megakaryocytes, and did not inhibit endomitosis of human megakaryocytes in immunodeficient NOD/Shi-*scid*/IL-2R ^{null} (NOG) mice transplanted with human CD34 cells (hu-NOG). We also demonstrated that a novel thrombopoietin mimetic, NIP-004, was effective for treating IFN- –induced thrombocytopenia in hu-NOG mice. From ultrastructural study, IFN- inhibited the maturation of demarcation membranes in megakaryocytes, although NIP-004 prevented the inhibitory effects of IFN- . These results defined the pathogenesis of IFN- –induced thrombocytopenia and suggested possible future clinical applications for thrombopoietin mimetics. (Blood. 2008;112: 542-550)

Introduction

Human interferon (IFN)- is the standard treatment for patients with chronic hepatitis C.[1,2] It is well known that chronic hepatitis C can lead to liver cirrhosis and hepatocellular carcinoma; the risk of progression to cirrhosis within 5 years is approximately 40%.[3] Among patients with compensated liver cirrhosis, the probability of its transition to decompensated cirrhosis and hepatocellular carcinoma within 5 years is approximately 20% and 10%, respectively.[4,5] Thus, it is important for chronic hepatitis C patients to receive IFN- treatment to prevent malignant transformation by eradicating hepatitis C virus.[6-11] However, IFN- –induced thrombocytopenia often leads to dose reduction or discontinuation of IFN- therapy. In particular, it is difficult to treat patients with advanced cirrhosis by IFN- because often these patients also have severe thrombocytopenia.

Several studies have suggested that IFN- induces thrombocytopenia by inhibiting the proliferation of human megakaryocytes, as the number of colony-forming units of megakaryocytes (CFU-MK) is reduced by relatively high concentrations of IFN- in vitro.[12-15] In clinical studies, however, the administration of human IFN- to patients with chronic hepatitis, solid tumors, and myeloproliferative disorders does not affect the number of megakaryocytes in bone marrow.[16-19] We speculate that this discrepancy is caused by differences in the dose of IFN- and hematopoietic microenvironment between CFU-MK in vitro assays and in vivo studies. Clinical studies have also proposed autoimmune reaction and capillary sequestration as causes of IFN- –induced thrombocytopenia.[18,20-22] Megakaryocytes differentiate from hematopoietic stem cells and undergo endomitosis followed by cytoplasmic maturation.[23,24] In endomitosis, megakaryocytes repeat DNA replication without cytokinesis to develop polyploidy. At the stage of cytoplasmic maturation in megakaryocytes, both the demarcation membrane system and granules develop, which enlarges the cell body. At the final stage of megakaryopoiesis, mature megakaryocytes extend thin protrusions called proplatelets, and their tips are released into the circulation as platelets. The lack of a suitable experimental animal model of human megakaryopoiesis has hampered the study of the mechanism of IFN- –induced thrombocytopenia. We recently developed a new experimental animal model of human megakaryopoiesis using immunodeficient nonobese diabetic (NOD)/Shi-*scid*/IL-2R ^{null} (NOG) mice transplanted with human CD34 cells (hu-NOG mice).[25] This prompted us to undertake this study, which investigates the mechanism of human IFN- –induced thrombocytopenia.

Thrombopoietin (TPO) is a lineage-specific cytokine that regulates both proliferation and differentiation of megakaryocytes.[26] The receptor for TPO is c-Mpl and *c-mpl*–deficient mice demonstrated severe thrombocytopenia, with an 85% reduction in the number of platelets and megakaryocytes.[27] Although several clinical trials of TPO have demonstrated that recombinant human (rh) TPO and pegylated recombinant human megakaryocyte growth and development factor (PEG-rhMGDF)

Submitted November 30, 2007; accepted April 6, 2008. Prepublished online as *Blood* First Edition paper, June 3, 2008; DOI 10.1182/blood-2007-12-125906.

*A.Y. and T.N. contributed equally to this study and should be regarded as co–first authors.

The publication costs of this article were defrayed in part by page charge payment. Therefore, and solely to indicate this fact, this article is hereby marked "advertisement" in accordance with 18 USC section 1734.

are effective for treating thrombocytopenia associated with nonmyeloablative chemotherapy, some individuals treated with PEG-rhMGDF have demonstrated thrombocytopenia because of the development of neutralizing antibodies to endogenous TPO,[28,29] which led to a clinical trial of rhTPO and PEG-rhMGDF being aborted.

Recently, second-generation of thrombopoietic growth factors such as TPO peptide (AMG 531) and TPO nonpeptide mimetics (eltrombopag, AKR501) have been shown to increase platelet counts in healthy volunteers and patients with chronic idiopathic thrombocytopenic purpura.[30-33] We recently created a novel TPO receptor activator, NIP-004.[25] NIP-004 is a nonpeptidyl mimetic of TPO and induces colony formation of megakaryocytes from human CD34 hematopoietic cells by activating the human TPO receptor. Interestingly, NIP-004 displays strict species specificity for the human TPO receptor, as the histidine residue in the transmembrane domain of human TPO receptor is critical for NIP-004 to induce intracellular signaling.[25]

In this study, we use human primary megakaryocytes to demonstrate that IFN- inhibits maturation of demarcation membranes and platelet production, but not endomitosis. We also confirm, in a hu-NOG mouse model, that NIP-004 is effective for the treatment of IFN- –induced thrombocytopenia.

Methods

Reagents and cells

Cytokines, including recombinant human IFN- 2b (Imgenex, San Diego, CA), human PEG-IFN- 2b (PEG-Intron; Schering Plough, Kenilworth, NJ), and recombinant human TPO (R&D Systems, Minneapolis, MN) were obtained as indicated. NIP-004 was chemically synthesized at Nissan Chemical Industries (Chiba, Japan).[25] Human bone marrow– and cord blood–derived CD34 cells were purchased from Lonza Walkersville (Walkersville, MD).

CFU assay

CFU-MK assay was performed using a MegaCult-C (StemCell Technologies, Vancouver, BC). A total of 5 10^3 human bone marrow–derived CD34 cells were cultured in collagen-based medium containing rhTPO in combination with rhIFN- 2b, in a CO_2 incubator for 10 days. After fixation, megakaryocytes were visualized with antihuman CD41a antibody using alkaline phosphatase staining. Nuclei were counterstained with Evans blue. Stained colonies were counted under a microscope (BX51; Olympus, Tokyo, Japan), and colonies, including one or more CD41a-positive megakaryocytes more than 100 m in diameter were counted separately.

Proplatelet formation assay

Human bone-marrow-derived CD34 cells were cultured at 10^5 cells/mL in StemSpan serum-free expansion medium (StemCell Technologies) supplemented with 40 g/mL low density lipoprotein and 10 ng/mL TPO at 37°C with 5% CO_2 for 7 days. Megakaryocytes were enriched by velocity sedimentation, as described by Choi et al.[34] Briefly, cultured cells were suspended in CATCH buffer (phosphate-buffered saline with 13.6 mM sodium citrate, 2.2 M prostaglandin E1, 1 mM theophylline, and 1 mM glucose) at 5 10^5 cells/mL and were subjected to a 2-step bovine serum albumin (BSA) gradient, 2.41% (2.5 mL) and 4.83% (5.0 mL), at 1 g for 1.5 hours at room temperature. Large megakaryocytes were collected from the bottom layer and cultured with 10 ng/mL of TPO in combination with 0 to 10 ng/mL of IFN- 2b in 96-well plates for 4 to 6 days. Proplatelet-displaying megakaryocytes were defined as cells that exhibited one or more filament-like protrusions with tips, and were counted under an inverted microscope at a magnification of 200. We counted 500 cells and calculated the percentage of megakaryocytes with proplatelets. Three independent experiments were performed using 3 different donor cells.

Fluorescent Images

Human CD34 bone marrow–derived cells were cultured with 10 ng/mL TPO for 7 days. Large megakaryocytes were collected by BSA velocity sedimentation and cultured with 10 ng/mL TPO in combination with 0 or 10 ng/mL IFN- 2b on poly-D-lysine culture slide (BD Biosciences, San Jose, CA) for 5 days. Culture-derived cells were fixed with 1% paraformaldehyde for 15 minutes at room temperature and then permeabilized with 0.2% Triton X-100 for 5 minutes at room temperature. Cells were blocked with 2% fetal bovine serum in phosphate-buffered saline for 1 hour and stained with Alexa Fluor 555-conjugated -tubulin (9F3) antibody (Cell Signaling Technology, Danvers, MA) overnight at 4°C. Images were captured by confocal laser and fluorescence microscopy. Single-photon confocal fluorescence images were collected using a Zeiss LSM510 (Carl Zeiss, Welwyn Garden City, United Kingdom) coupled to an inverted microscope (Zeiss Axiovert 100) equipped with a 63 /1.4 numeric aperture oil objective. Alexa Fluor 555 was excited at 535 nm and emissions were collected above 560 nm.

Real-time quantitative reverse-transcriptase polymerase chain reaction

Total RNA was extracted using a RNeasy Mini Extraction Kit (Qiagen, Hilden, Germany), and 0.5 g of RNA was subjected to reverse transcription using a SuperScript First-Strand Synthesis System for reverse-transcriptase polymerase chain reaction (RT-PCR; Invitrogen, Carlsbad, CA). TaqMan Gene Expression Assays were used for RT-PCR following the manufacturer's instructions. The plate was run on an Applied Biosystems 7500 Fast Real-Time PCR System (Applied Biosystems, Foster, CA). All reactions were normalized with the respective hypoxanthine ribosyl transferase (HPRT) mRNA levels, and experiments were performed in triplicate. HPRT was chosen as an endogenous control from the results using a TaqMan Human Endogenous Control Plate (Applied Biosystems).

In vivo assay

Immunodeficient NOG mice were created at the Central Institute for Experimental Animals (Kawasaki, Kanagawa, Japan) and were maintained under specific pathogen-free conditions.[25] NOG mice were provided with sterile water containing prophylactic neomycin sulfate (Invitrogen). After 2.4 Gy irradiation, 10^5 human umbilical cord blood–derived CD34 cells were intravenously injected into NOG mice. Three months later, PEG-IFN- 2b was subcutaneously administered into the NOG mice 3 times weekly for 3 weeks. After we confirmed PEG-IFN- 2b–induced thrombocytopenia, NIP-004 was administered in combination with 30 g/kg PEG-IFN- 2b for an additional 4 weeks. The number of human platelets was measured by flow cytometry using species-specific antibodies against human CD41 and Flow-Count Fluorospheres (Beckman Coulter, Fullerton, CA). For measuring the life span of human platelets in hu-NOG mice, in vivo biotinylation was performed as previously described.[35] Briefly, 3 mg sulfo-NHS-LC-biotin (Pierce Chemical, Rockford, IL) was dissolved in 300 L saline, and 150 L of the solution was injected intravenously. Blood from biotinylated mice was stained by antibodies against human CD41a and CD42b and phycoerythrin Texas red (ECD)–labeled streptavidin (BD Biosciences PharMingen, San Diego, CA). Samples were analyzed by flow cytometry to obtain the number of biotinylated human platelets. From plots of the number of biotinylated human platelets vs time, an estimate of the life span was obtained by linear extrapolation. Animal experiments were conducted according to the guidelines for animal experiments[36] of the Japanese Association for Laboratory Animal Science. All experimental protocols were approved by the ethics review committees for animal experiments of Keio University and Nissan Chemical Industries.

Flow cytometry

Multicolor flow cytometry was performed using an EPICS-XL flow cytometer (Beckman Coulter) as previously described.[25] Antibodies used in this study were as follows: antihuman CD33-fluorescein isothiocyanate (FITC), CD3-FITC, CD41a-FITC, CD71-FITC, CD42a-FITC, CD34-phycoerythrin (PE), CD41a-PE, glycophorin A (GPA)-PE, CD42b-PE, CD19-PE, CD45-ECD, CD41a-PE 5 succinimidylester (PC5), CD38-PC5, antimurine CD45-FITC, and CD41-FITC. Antibodies against antihuman

CD45-ECD were purchased from Immunotech (Marseille, France). Other antibodies were purchased from BD Biosciences PharMingen. The actual number of platelets and bone marrow cells in hu-NOG mice and culture-derived platelets was measured by flow cytometry using the indicated species-specific antibodies and Flow-Count Fluorospheres. To analyze human megakaryocyte ploidy, culture-derived cells and bone marrow cells from hu-NOG mice were stained with antihuman CD41a-PE antibody and fixed with 1% paraformaldehyde. Fixed cells were treated with Tween 20 and 7-amino-actinomycin D (7-AAD) dye (Immunotech) followed by 2-color cytometric analysis.

Electron microscopy

Human bone marrow–derived CD34 cells were cultured with 10 ng/mL of TPO for 7 days. Large megakaryocytes were collected by BSA velocity sedimentation and cultured with 10 ng/mL TPO in combination with 0 or 10 ng/mL IFN- 2b and 0 or 1 g/mL NIP-004 for 5 days. Culture-derived cells were fixed in 2% glutaraldehyde in 0.1 M phosphate buffer (pH 7.4) for 60 minutes at 4°C. The samples were washed, then fixed with 1% osmium tetroxide in 0.1 M phosphate buffer for 60 minutes at 4°C, dehydrated with a graded ethanol series, and embedded in Epon (TAAB Laboratories, Aldermaston, United Kingdom), as described previously.[37] Ultrathin sections were prepared, stained with uranyl acetate and lead citrate, and then examined with a JEM1200EX transmission electron microscope (JEOL, Tokyo, Japan) at an accelerating voltage of 80 kV. To evaluate the differentiation of megakaryocytes, we divided megakaryocytes into 3 types according to their developmental stage. We defined immature megakaryocytes, with a large round nucleus but no demarcation membrane system, as type 1 megakaryocytes. Type 2 megakaryocytes were the intermediate stage between types 1 and 3 megakaryocytes. Type 3 were fully matured megakaryocytes, in which the nucleus was pushed to the side of the cell, cytoplasm was abundant, and the area of the demarcation membrane system was more than 20% of the cell body. We counted more than 100 megakaryocytes by electron microscopy and calculated the percentage of each type.

Statistical analysis

Comparisons among groups were performed by Student *t* test. All tests were 2-sided and *P* less than .05 was considered significant.

Results

Colony-forming assay of megakaryocytes using human CD34 hematopoietic stem cells

To investigate how IFN- reduces the number of platelets, we performed colony-forming assays of megakaryocytes using human bone marrow–derived CD34 cells. IFN- 2b at 1 and 10 ng/mL reduced the number of CFU-MK by 13% and 18%, respectively; however, these decreases were not statistically significant (Figure 1A left panel). The average CFU-MK was calculated from 3 independent experiments. We noticed that the size of megakaryocytes treated with IFN- was smaller than that without IFN- ; thus, we counted the number of CFU-MK that included one or more megakaryocytes more than 100 m in diameter. IFN- 2b at 1 and 10 ng/mL significantly reduced the number of CFU-MK that included at least one large megakaryocyte by 42% and 67%, respectively (*P* .05, n 3; Figure 1A right panel).

The effects of IFN- 2b on DNA ploidy of human megakaryocytes in vitro

To investigate whether the reduction of megakaryocyte cell size by IFN- 2b was caused by the inhibition of endomitosis, we measured DNA ploidy of megakaryocytes by flow cytometry.

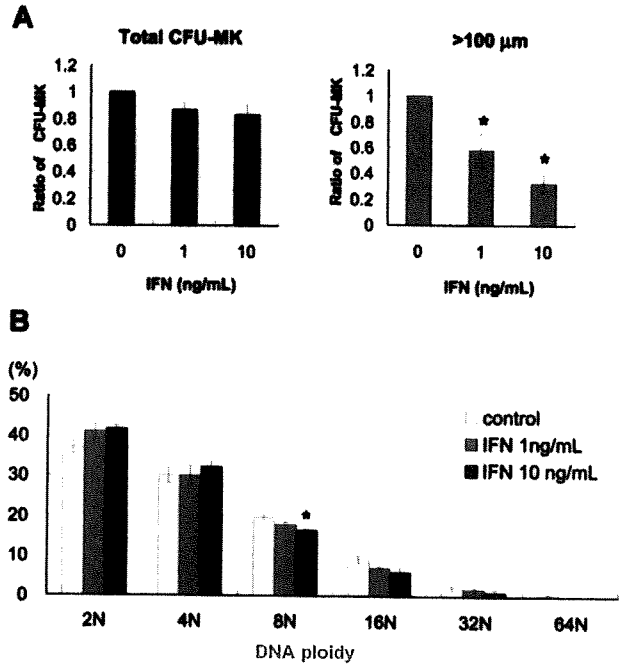

Figure 1. Effects of IFN- 2b on colony formation and DNA ploidy of primary human megakaryocytes. (A) Human bone marrow–derived CD34 cells were treated with 10 ng/mL TPO and 0, 1, or 10 ng/mL IFN- 2b for 10 days. (Left graph) Total number of CFU-MK. The average number was calculated from 3 independent experiments. (Right graph) Number of CFU-MK that included one or more megakaryocytes more than 100 m in diameter. Diameters were measured under a microscope using a microscale within an eyepiece. Data are means plus or minus SEM from the results of 3 independent experiments (*P* .05 vs 0 ng/mL IFN- 2b). (B) Effects of IFN- 2b on DNA ploidy of megakaryocytes in vitro. Human bone marrow–derived CD34 cells were cultured with 10 ng/mL of TPO in combination with 0, 1, or 10 ng/mL IFN- 2b. Megakaryocytes were stained with antihuman CD41a-PE antibody and 7-AAD dye, and examined by 2-color cytometry. Data are means plus or minus SEM from the results of 3 independent experiments (*P* .05 vs 0 ng/mL IFN- 2b).

We cultured human bone marrow–derived CD34 cells with 10 ng/mL of TPO in combination with 0, 1, and 10 ng/mL IFN- 2b for 10 days and analyzed DNA ploidy of megakaryocytes. IFN- 2b did not alter DNA ploidy of human megakaryocytes except 8N with 10 ng/mL IFN- 2b (*P* .05, n 3; Figure 1B). Three independent experiments were performed to confirm reproducibility.

IFN- 2b inhibited platelet production in vitro

As we found that IFN- 2b did not inhibit endomitosis of megakaryocytes, we investigated the effects of IFN- 2b on proplatelet formation (PPF) and platelet production, using primary human megakaryocytes. We defined PPF as megakaryocytes that displayed at least one filament-like extension with tips, and counted 500 cells in 3 independent experiments (Figure 2). IFN- 2b significantly inhibited PPF in a dose-dependent manner (Figure 2A). IFN- 2b at 1 and 10 ng/mL inhibited PPF by 39% and 60%, respectively, on day 12, and by 47% and 61%, respectively, on day 13 (*P* .05, n 3).

We also counted the number of culture-derived platelets by flow cytometry. The platelets produced from primary human megakaryocytes in the culture supernatant were collected and stained with antihuman CD41a and CD42a antibodies. IFN- 2b at 1 and 10 ng/mL reduced the number of culture-derived platelets by 60% and 73%, respectively, on day 13 (*P* .05, n 3; Figure 2B). We performed 3 independent experiments using 3 different donors to

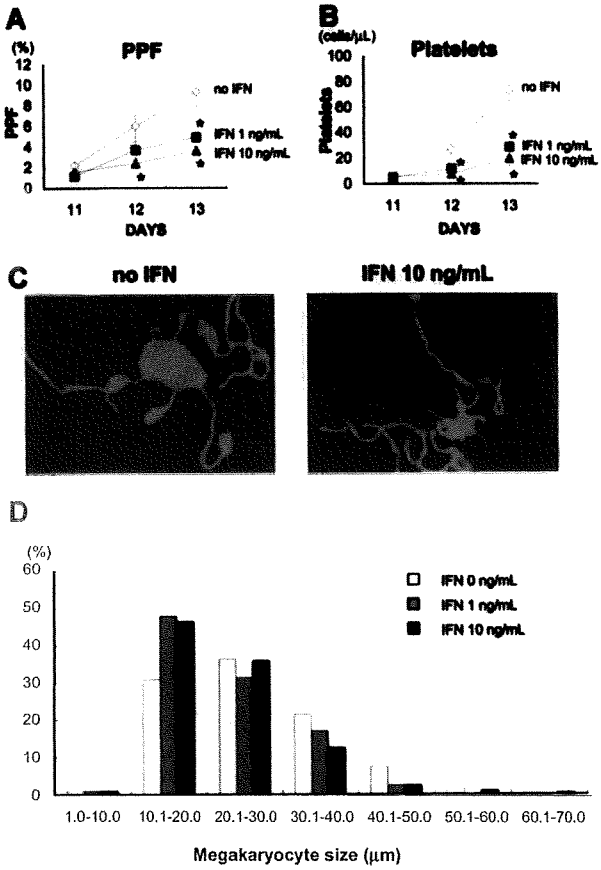

Figure 2. IFN- 2b inhibited proplatelet formation (PPF) and production of platelets from primary human megakaryocytes. Human bone marrow–derived CD34 cells were cultured with 10 ng/mL TPO for 7 days. After collecting large megakaryocytes using velocity sedimentation, we maintained the cells with 10 ng/mL TPO in combination with 10 ng/mL IFN- 2b in 96-well plates for 6 days. (A) The numbers of megakaryocytes displaying PPF were counted under an inverted microscope at 200. We counted 500 cells for each sample 3 times. Data are means plus or minus SEM (n 3). (B) Platelets in the culture supernatant of primary human megakaryocytes were stained with antihuman CD41a and CD42a antibodies and counted by flow cytometry. Data are means plus or minus SEM (n 3). (C) A representative picture of PPF with TPO and TPO plus IFN- 2b. Megakaryocytes were stained with Alexa Fluor 555-conjugated -tubulin (9F3) antibody on day 12 and photographed under confocal laser microscopy. (D) IFN- 2b decreased the size of human megakaryocytes. Megakaryocytes were collected on day 13 and spun down on to glass slides. After staining with Wright-Giemsa solution, the diameters of the megakaryocytes were measured with a microscope using a scale within an eyepiece.

confirm reproducibility. IFN- 2b did not change the appearance of proplatelets, such as branches, shafts, and tips (Figure 2C), although it significantly inhibited the percentage of megakaryocytes demonstrating PPF and the count of culture-derived platelets (Figure 2A,B). Because PPF and the number of platelets reflect the development of the demarcation membrane system in cytoplasm, we measured the size of each megakaryocyte on day 13; these were then cytospun on to glass slides and stained with Giemsa solution (Figure 2D). IFN- 2b at 1 and 10 ng/mL decreased the mean size of human megakaryocytes from 27.3 (0 ng/mL) to 23.5 and 23.7 m, respectively.

IFN- 2b suppressed mRNA expression of transcription factors regulating late-stage megakaryopoiesis

To clarify the molecular mechanism of how IFN- 2b inhibits cytoplasmic maturation and platelet production in megakaryocytes, we analyzed mRNA expression of GATA-1, p45$^{NF\text{-}E2}$, MafG, and VWF using quantitative PCR. The transcription factors GATA-1, p45$^{NF\text{-}E2}$, and MafG are reported to be involved in late-stage megakaropoiesis.[38-40] VWF in -granules is a marker of cytoplasmic maturation of megakaryocytes.[41] We extracted total RNA from human megakaryocytes that were cultured with 10 ng/mL TPO and 0, 1, and 10 ng/mL IFN- 2b for 5 days after BSA-based velocity sedimentation. The mRNA expression of these transcription factors was inhibited by IFN- 2b in a dose-dependent manner (Figure 3). IFN- 2b at 10 ng/mL suppressed the mRNA expression levels of GATA-1, p45$^{NF\text{-}E2}$, MafG, and VWF by 70%, 58%, 55%, and 68%, respectively (Figure 3).

IFN- 2b decreased the number of human platelets without affecting the number and DNA ploidy of human megakaryocytes in hu-NOG mice

To evaluate the effects of human IFN- 2b on human megakaryopoiesis in vivo, we transplanted human umbilical cord blood–derived CD34 cells into NOG mice. We administered PEG-IFN- 2b at 10 and 30 g/kg to hu-NOG mice 3 times weekly for 7 weeks and found that IFN- 2b significantly reduced the number of human platelets by 59% and 68%, respectively, compared with that in the control mice (Figure 4A left panel). The number of murine platelets was not changed by PEG-IFN- 2b because human IFN- 2b does not affect murine cells (Figure 4A right panel). To precisely analyze the effects of PEG-IFN- 2b on human hematopoiesis, we counted the number in each lineage of human hematopoietic cells in bone marrow of hu-NOG mice, using flow cytometry (Table 1). PEG-IFN- 2b at 10 or 30 g/kg 3 times weekly for 7 weeks did not reduce the number of human CD41 megakaryocytes. By contrast, PEG-IFN- 2b significantly reduced the number of human CD45 CD33 myeloid cells and CD45 CD71 GPA erythroblasts in the bone marrow of hu-NOG mice (Table 1). None of the lineages of murine hematopoietic cells was changed by PEG-IFN- 2b (data not shown) because of species specificity. As PEG-IFN- 2b decreased the number of human platelets in hu-NOG mice, we evaluated the effects of PEG-IFN- 2b on endomitosis of human megakaryocytes by flow cytometry. PEG-IFN- 2b had no effects on DNA ploidy of human megakaryocytes in hu-NOG mice (Figure 4B), which was consistent with the data from in vitro experiments.

IFN- did not promote the clearance of human platelets in hu-NOG mice

To exclude the possibility that IFN- may facilitate the clearance of human platelets in hu-NOG mice by activating human platelets or macrophages, we measured the life span of human platelets in hu-NOG mice by labeling them with biotin. When hu-NOG mice were treated with PEG-IFN- 2b 30 g/kg 3 times weekly for 3 weeks, the number of human platelets was decreased by 47%, and the life span of human platelets was 6.1 (0.2) days (mean SEM, n 5). In control hu-NOG mice treated with vehicle, the life span of human platelets was 6.0 (0.2) days (n 4). Because the life span of human platelets was not changed by IFN- 2b treatment, we concluded that IFN- 2b decreased human platelet count by inhibiting platelet production, but not by promoting their clearance.

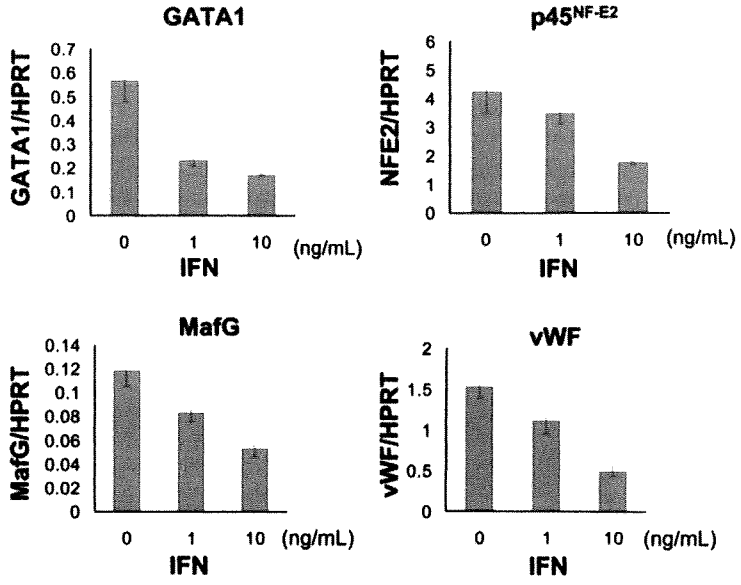

Figure 3. IFN- 2b suppressed expression of transcription factors regulating late-stage megakaryopoiesis. Human bone marrow–derived CD34 cells were incubated with 10 ng/mL TPO for 7 days. Large megakaryocytes were enriched by velocity sedimentation, followed by 6 days of incubation with 10 ng/mL TPO and 0, 1, or 10 ng/mL IFN- 2b. Total RNA was extracted from these megakaryocytes. TaqMan Gene Expression Assay was used for real-time PCR. All data were standardized with respective HPRT mRNA levels. Data are means plus or minus SEM of 3 samples.

NIP-004 was effective for treating IFN- –induced thrombocytopenia in hu-NOG mice

We recently developed a novel nonpeptidyl Mpl activator, NIP-004, that can induce formation of CFU-MK and increase human platelets in hu-NOG mice.[25] To evaluate the effects of NIP-004 on IFN- –induced thrombocytopenia, we administered NIP-004 30 mg/kg per day to hu-NOG mice after 3 weeks of treatment with PEG-IFN- 2b. NIP-004 restored human platelet

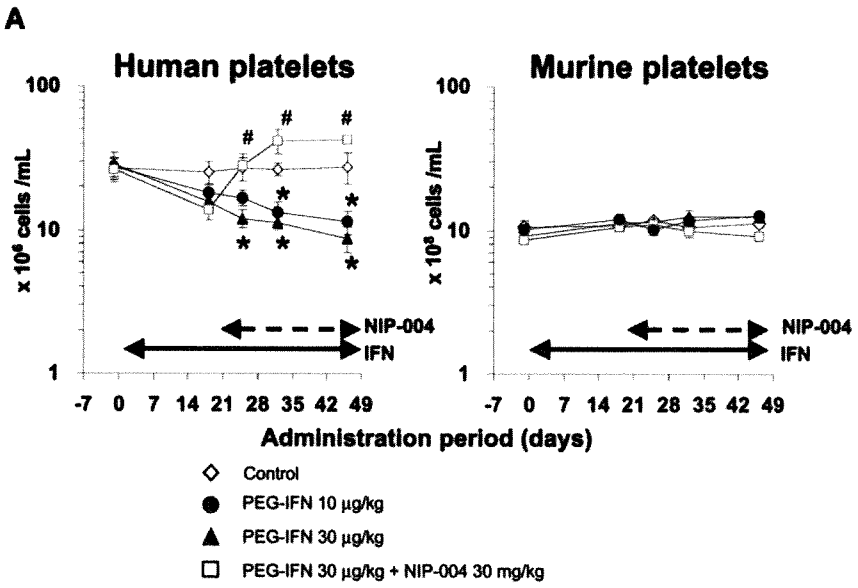

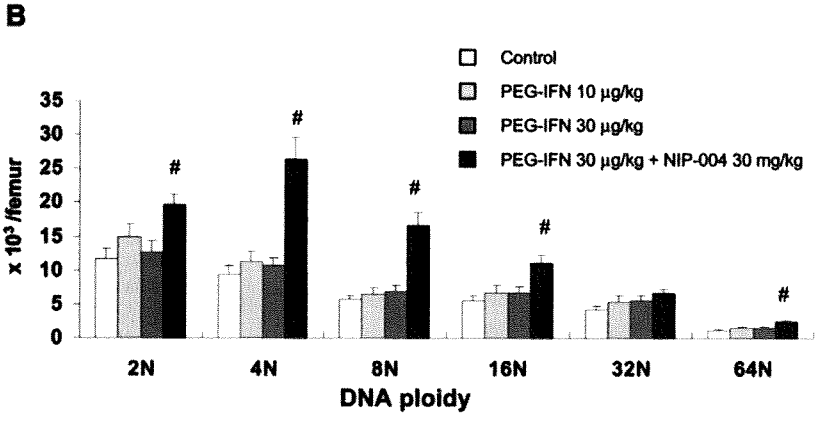

Figure 4. Effects of IFN- 2b and NIP-004 on human platelets and megakaryocytes in hu-NOG mice. Human cord blood–derived CD34 cells were transplanted into immunodeficient NOG mice (hu-NOG). Three months after transplantation, human PEG-IFN- 2b was administered to hu-NOG mice 3 times weekly for 7 weeks. NIP-004 was administered daily to hu-NOG mice for 4 weeks, 3 weeks after initial treatment with PEG-IFN- 2b. (A) The number of human platelets was decreased by PEG-IFN- 2b in a dose-dependent manner. NIP-004 reversed the decrease in human platelets. By contrast, the number of murine platelets in hu-NOG mice was not changed because of the species specificity of human PEG-IFN- 2b and NIP-004. (B) DNA ploidy of human megakaryocytes in hu-NOG mice. Bone marrow cells collected from hu-NOG mice were stained with antihuman CD41a antibody and 7-AAD dye. The number of each ploidy in human megakaryocytes was measured by flow cytometry using Flow-Count Fluorospheres. Data are means plus or minus SEM from 5 mice (*P .05 vs control; #P .05 vs PEG-IFN- 2b 30 g/kg).

Table 1. Cell counts of each human hematopoietic lineage in bone marrow of hu-NOG mice

Lineage	Control, n 5	IFN 10 g/kg, n 5	IFN 30 g/kg, n 5	IFN 30 g/kg; NIP-004 30 mg/kg, n 5
Total white blood cells, 10^6	6.5 0.5	3.9 0.6	4.7 0.7	5.4 0.4
Megakaryocytes, 10^4	3.9 0.5	4.7 0.5	4.7 0.5	8.2 0.8*†
Myeloid cells, 10^6	2.5 0.3	0.9 0.1*	1.0 0.1*	2.0 0.2
Erythroblasts, 10^4	6.9 1.5	1.1 0.5*	0.2 0.1*	0.3 0.1*
Progenitor cells, 10^5	3.2 0.9	3.1 0.5	3.9 0.8	4.4 0.3
B cells, 10^6	3.2 0.3	2.2 0.4	3.0 0.7	2.2 0.2
T cells, 10^5	2.6 0.2	1.6 0.2	1.3 0.3	1.8 0.2

Data are means (SEM) of cells/femur for 5 mice. Bone marrow cells were collected from the femurs of NOG mice transplanted with human umbilical cord blood–derived CD34 cells (hu-NOG). The number in each cell lineage was measured by flow cytometry using lineage-specific antibodies and Flow-Count Fluorospheres. PEG-IFN- 2b and NIP-004 were administered using the same protocol as described in Figure 4. Each lineage-specific marker was indicated as follows: total white blood cells, CD45 ; megakaryocytes, CD41 ; myeloid cells, CD45 CD33 ; erythroblasts, CD45 CD71 GPA ; progenitor cells, CD45 CD34 ; B cells, CD45 CD38 CD19 ; T cells, CD45 CD38 CD3 .

*P .01 versus control.

†P .01 versus PEG-IFN- 2b 30 g/kg single treatment.

counts in hu-NOG mice undergoing treatment with PEG-IFN- 2b 30 g/kg (Figure 4A). NIP-004 30 mg/kg per day significantly increased the number of human megakaryocytes in all DNA ploidy classes but the 32N class with statistically significant differences in hu-NOG mice (Figure 4B; Table 1). NIP-004 did not affect murine megakaryopoiesis because it does not work for murine cells, as previously described (Figure 4A right panel, and data not shown).[25]

IFN- 2b inhibited the development of the demarcation membrane system in human megakaryocytes

To analyze the effects of IFN- 2b on cytoplasmic maturation of human megakaryocytes, ultrastructural study using electron microscopy was performed. When human megakaryocytes were cultured with TPO, almost half the cells had a lobulated nucleus and abundant cytoplasm with a mature demarcation membrane system (Figure 5Avii). The percentages of each type of megakaryocyte were 13% for type 1 (immature; Figure 5Ai), 44% for type 2 (intermediate; Figure 5Aiv), and 43% for type 3 (mature; Figure 5Avii). When megakaryocytes were cultured with TPO and IFN- 2b, the percentages of each type were 12% for type 1 (Figure 5Aii), 63% for type 2 (Figure 5Av), and 25% for type 3 (Figure 5Aviii). The percentage of type 3 megakaryocytes was reduced by 42% and type 2 was increased by 43% with IFN- 2b compared with controls (Figure 5B). For each type, we observed no obvious effects of IFN- 2b on the number of granules or the appearance of mitochondria and nuclei. We performed 4 experiments separately to confirm reproducibility and to calculate the average and standard deviation (Figure 5B). These results indicated that IFN- 2b inhibited the maturation of the demarcation membrane system in primary human megakaryocytes. Next, we tested whether NIP-004 inhibited the effects of IFN- 2b on the maturation of the demarcation membrane system. When megakaryocytes were cultured with TPO plus IFN- 2b plus NIP-004, the percentages of each type were 7% for type 1 (Figure 5Aiii), 46% for type 2 (Figure 5Avi), and 47% for type 3 (Figure 5Aix). These results indicated that NIP-004 prevented the inhibitory effects of IFN- 2b on the maturation of the demarcation membrane system in primary human megakaryocytes (Figure 5B). We performed 2 experiments separately to confirm reproducibility (P .05).

Discussion

IFN- has been proposed to induce thrombocytopenia mainly by inhibiting proliferation and maturation of megakaryocytes.[12-15] Autoimmune-based destruction of platelets[20,21] and capillary sequestration have also been proposed as causes of IFN- –induced thrombocytopenia.[18,20-22] In this study, we used primary human megakaryocytes to successfully demonstrate that IFN- 2b inhibited cytoplasmic maturation and platelet production of megakaryocytes, but not proliferation and endomitosis. Leukemia cell lines do not demonstrate PPF or produce platelets; thus, in this study, we used human primary megakaryocytes for in vitro assays and in vivo models to analyze the mechanism of IFN-induced thrombocytopenia.

Because IFN- 2b did not decrease the number of CFU-MK using human CD34 cells, we speculate that IFN- 2b does not inhibit the commitment of CD34 cells to the megakaryocytic lineage and proliferation of immature megakaryocytes, but it does inhibit late-stage megakaryopoiesis. PPF and platelet production represent late-stage megakaryopoiesis; therefore, we used human primary megakaryocytes to analyze the effects of IFN- 2b on PPF and platelet production. As expected, IFN- 2b significantly inhibited PPF and platelet production in vitro. We also evaluated cytoplasmic maturation of megakaryocytes by electron microscopy. IFN- 2b reduced by half the percentage of type 3 megakaryocytes with a fully matured demarcation membrane system. This result suggested that IFN- 2b inhibited maturation of the demarcation membrane system in megakaryocytes. Demarcation membranes are thought to be the membrane reservoir for formation of proplatelets. The precise molecular mechanisms of how IFN- 2b inhibits the maturation of demarcation membranes and platelet formation remain to be elucidated. Inhibition of maturation of the demarcation membrane system by IFN- 2b may be involved in the impairment of PPF. This might affect the inhibition of PPF and platelet production.

IFN- 2b did not reduce the number of human megakaryocytes, although it significantly reduced the number of human platelets in hu-NOG mice. As well, IFN- 2b did not alter DNA ploidy of human megakaryocytes in the bone marrow of hu-NOG mice, indicating that IFN- 2b inhibited late-stage megakaryopoiesis. Previous clinical studies have demonstrated that IFN- reduces the

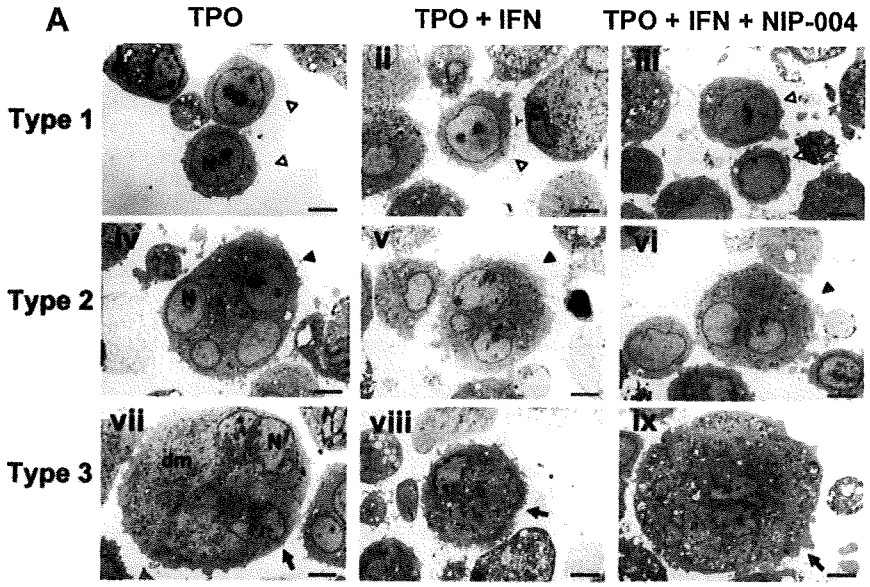

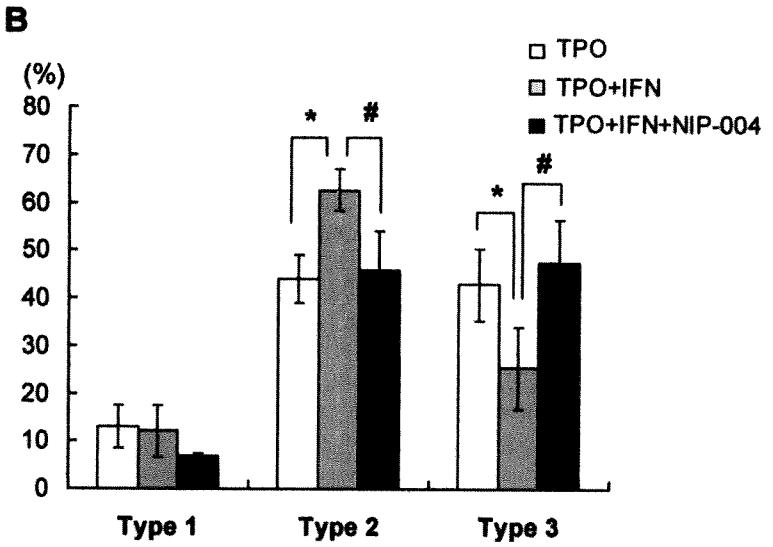

Figure 5. Ultrastructure of megakaryocytes cultured with or without IFN- 2b. (A) Ultrastructures of representative human megakaryocytes cultured with 10 ng/mL TPO, 10 ng/mL TPO plus 10 ng/mL IFN- 2b, and 10 ng/mL TPO plus 10 ng/mL IFN- 2b plus 1 g/mL NIP-004. represent type 1 immature megakaryocytes (i-iii); Š, type 2 intermediate megakaryocytes (iv-vi); →, type 3 fully matured megakaryocytes (vii-ix). The definition of each type is in "Electron microscopy." Original magnification, 3000. Scale bar represents 4 m. N indicates nucleus; Dm, demarcation membranes. (B) The percentage of each type of megakaryocytes. IFN- 2b decreased type 3 megakaryocytes and increased type 2 compared with control (TPO) with statistically significant differences, indicating that IFN- 2b inhibits the development of the demarcation membrane system of megakaryocytes. Data are means plus or minus SD from the results of 4 independent experiments (*P .05 vs TPO). NIP-004 prevented the inhibitory effects of IFN- 2b on the development of the demarcation membrane system of megakaryocytes. Data are means plus or minus SD from the results of 2 independent experiments (#P .05 vs TPO IFN).

number of platelets without decreasing the number of megakaryocytes in patients with chronic hepatitis, solid tumors, and myeloproliferative disorders,[16-19] which is consistent with our results. IFN- has been reported to significantly decrease the size of megakaryocytes in patients with essential thrombocythemia and polycythemia vera.[17,19] These clinical observations also support our conclusion that IFN- inhibits cytoplasmic maturation of megakaryocytes but not endomitosis.

Because it is possible that IFN- promotes the consumption of platelets in hu-NOG mice, we measured the life span of human platelets in hu-NOG mice and found that IFN- 2b did not shorten the life span. Therefore, we concluded that IFN- 2b induced thrombocytopenia by inhibiting platelet production, but not by facilitating the consumption of platelets. GATA-1 and NF-E2 are essential transcription factors in late-stage megakaryopoiesis. Lineage-selective GATA-1 knockout mice have abnormal megakaryocytes with a small cytoplasm and few granules.[38] GATA-1 knockdown megakaryocytes are small, with low ploidy.[42] NF-E2 is composed of 2 basic leucine zipper subunits of $p45^{NF-E2}$ and p18 and is one of the small Maf proteins that includes MafG.[43] $p45^{NF-E2}$ knockout megakaryocytes do not have platelet formation and granules, but their DNA ploidy is increased in compensation.[40] MafG-null mutant mice exhibit thrombocytopenia and impairment of PPF.[39,44] We demonstrated that IFN- 2b suppressed mRNA expression levels of GATA-1, $p45^{NF-E2}$, and MafG in primary human megakaryocytes using quantitative PCR. Down-regulation of these transcription factors might be involved in inhibition of the cytoplasmic maturation of human megakaryocytes by IFN- . Ishida et al used murine megakaryocytes and reported that limitin and IFN- induce the expression of Daxx protein and phosphorylation of Crk adaptor protein.[45] IFN- –induced growth inhibition is also mediated by Crk in myeloid and erythroid progenitor cells, and by Daxx in B lymphoid progenitors.[46,47] Wang et al demonstrated that IFN- induces the expression of SOCS-1 transcription factor, which could blunt TPO-induced intracellular signaling in murine primary megakaryocytes.[12] IFN- activates JAK1 and TYK2 tyrosine kinses, which phosphorylate STAT1 and STAT2 transcription factors. Phosphorylated STAT1 and STAT2 form a complex

with IFN regulatory factor (IRF)-9, named IFN-stimulating gene factor 3. IFN-stimulating gene factor 3 migrates into the nucleus where it binds to the IFN-stimulated response element in the promoter region of hundreds of genes. STAT1/STAT1 homodimer mediates the alternative pathway by binding to IFN- activated sequence. To the best of our knowledge, no other study has demonstrated how IFN- decreases the expression of GATA-1, $p45^{NF\text{-}E2}$, and MafG. Further investigation will be needed to elucidate this mechanism.

NIP-004 is a novel TPO mimetic and can increase the number of human megakaryocytes and induce their maturation, accompanied by an increase in human platelets in hu-NOG mice.[25] We confirmed the effects of NIP-004 on IFN- -induced thrombocytopenia using hu-NOG mice in this study. NIP-004 increased the number of human megakaryocytes in hu-NOG mice treated with IFN- 2b. The dose of PEG-IFN- 2b in this study was higher than that used in clinical settings. Based on our preliminary data related to the pharmacokinetics of PEG-IFN- 2b in NOG mice, we found that clearance of PEG-IFN- 2b was 3 times faster than that in humans (data not shown). Therefore, we needed to inject PEG-IFN- 2b at higher doses to retain an effective concentration in NOG mice.

In conclusion, we demonstrated that IFN- 2b directly inhibited cytoplasmic maturation and platelet production, but not proliferation and endomitosis in human primary megakaryocytes. TPO mimetics might be useful for treating IFN-induced thrombocytopenia, and their clinical application might encourage physicians and patients to continue IFN therapy.

Acknowledgments

The authors thank Ms Asako Ikejima for technical assistance, Dr Kenneth Kaushansky for encouragement, and Dr Eri Matsuki for discussions.

Authorship

Contribution: A.Y. and T.N. performed the experiments, analyzed results, and compiled the figures; H.S. performed electron microscopy; M.I. and Y.O. contributed live mice; Y.I. controlled the data; and A.Y., T.N., and Y.M. designed the research and wrote the paper.

Conflict-of-interest disclosure: T.N. is an employee of Nissan Chemical Industries. Y.M. and Y.O. received research grants from Nissan Chemical Industries. The remaining authors declare no competing financial interests.

Correspondence: Yoshitaka Miyakawa, Division of Hematology, Department of Internal Medicine, Keio University School of Medicine, 35 Shinanomachi, Shinjuku, Tokyo 160-8582, Japan; e-mail: yoshi@sc.itc.keio.ac.jp.

References

1. Manns MP, McHutchison JG, Gordon SC, et al. Peginterferon alfa-2b plus ribavirin compared with interferon alfa-2b plus ribavirin for initial treatment of chronic hepatitis C: a randomized trial. Lancet. 2001;358:958-965.
2. Fried MW, Shiffman ML, Reddy KR, et al. Peginterferon alfa-2a plus ribavirin for chronic hepatitis C virus infection. N Engl J Med. 2002;347:975-982.
3. Tremolada F, Casarin C, Alberti A, et al. Long-term follow-up of non-A, non-B (type C) post-transfusion hepatitis. J Hepatol. 1992;16:273-281.
4. Fattovich G, Giustina G, Degos F, et al. Morbidity and mortality in compensated cirrhosis type C: a retrospective follow-up study of 384 patients. Gastroenterology. 1997;112:463-472.
5. Hu K-Q, Tong MJ. The long-term outcomes of patients with compensated hepatitis C virus-related cirrhosis and history of parenteral exposure in the United States. Hepatology. 1999;29:1311-1316.
6. Heathcote EJ, Shiffman ML, Cooksley WG, et al. Peginterferon alfa-2a in patients with chronic hepatitis C and cirrhosis. N Engl J Med. 2000;343:1673-1680.
7. Horoldt B, Haydon G, O'Donnell K, Dudley T, Nightingale P, Mutimer D. Results of combination treatment with pegylated interferon and ribavirin in cirrhotic patients with hepatitis C infection. Liver Int. 2006;26:650-659.
8. Helbling B, Jochum W, Stamenic I, et al. HCV-related advanced fibrosis/cirrhosis: randomized controlled trial of pegylated interferon -1a and ribavirin. J Viral Hepat. 2006;13:762-769.
9. Hofer H, Gurguta C, Bergholz U, Steindl-Munda P, Ferenci P. Standard interferon-alpha in combination with ribavirin for hepatitis C patients with advanced liver disease and thrombocytopenia. Wien Klin Wochenschr. 2006;118:595-600.
10. Shiffman ML, Biscinglie AMD, Lindsay KL, et al. Peginterferon alfa-2a and ribavirin in patients with chronic hepatitis C who have failed prior treatment. Gastroenterology. 2004;126:1015-1023.
11. Nishiguchi S, Kuroki T, Nakatani S, et al. Randomised trial of effects of interferon-alpha on incidence of hapatocellular carcinoma in chronic active hepatitis C with cirrhosis. Lancet. 1995;346:1051-1055.
12. Wang Q, Miyakawa Y, Fox N, Kaushansky K. Interferon-alpha directly represses megakaryopoiesis by inhibiting thrombopoietin-induced signaling through induction of SOCS-1. Blood. 2000;96:2093-2099.
13. Ganser A, Carlo-Stella C, Greher J, Völkers B, Hoelzer D. Effect of recombinant interferons alpha and gamma on human bone marrow-derived megakaryocytic progenitor cells. Blood. 1987;70:1173-1179.
14. Dukes PP, Izadi P, Jorge OA, Shore NA, Gomperts E. Inhibitory effects of interferon on mouse megakaryocytic progenitor cells in culture. Exp Hematol. 1980;8:1048-1056.
15. Mazur EM, Richtsmeier WJ, South K. Alpha-interferon: differential suppression of colony growth from human erythroid, myeloid, and megakaryocytic hematopoietic progenitor cells. J Interferon Res. 1986;6:199-206.
16. Ernstoff MS, Kirkwood JM. Changes in the bone marrow of cancer patients treated with recombinant interferon alpha-2. Am J Med. 1984;76:593-596.
17. Wadenvik H, Kutti J, Ridell B, et al. The effect of -interferon on bone marrow megakaryocytes and platelet production rate in essential thrombocythemia. Blood. 1991;77:2103-2108.
18. Sata M, Yano Y, Yoshiyama Y, et al. Mechanisms of thrombocytopenia induced by interferon therapy for chronic hepatitis B. J Gastroenterol. 1997;32:206-210.
19. Kreft A, Nolde C, Büsche G, Buhr T, Kreipe H, Georgii A. Polycythaemia vera: bone marrow histopathology under treatment with interferon, hydroxyurea and busulphan. Eur Haematol. 2000;64:32-41.
20. Dourakis SP, Deutsch M, Hadziyannis SJ. Immune thrombocytopenia and alpha-interferon therapy. J Hepatol. 1996;25:972-975.
21. Elefsiniotis IS, Pantazis KD, Fotos NV, Moulakakis A, Mavrogiannis C. Late onset autoimmune thrombocytopenia associated with pegylated interferon- -2b plus ribavirin treatment for chronic hepatitis C. J Gastroenterol Hepatol. 2006;21:622-623.
22. Dormann H, Krebs S, Muth-Selbach U, et al. Rapid onset of hematotoxic effects after interferon alpha in hepatitis C. J Hepatol. 2000;32:1041-1042.
23. Odell TT, Jackson C. Polyploidy and maturation of rat megakaryocytes. Blood. 1968;32:102-110.
24. Raslova H, Kauffmann A, Sekkai D, et al. Interrelation between polyploidization and megakaryocyte differentiation: a gene profiling approach. Blood. 2007;109:3225-3234.
25. Nakamura T, Miyakawa Y, Miyamura A, et al. A novel nonpeptidyl human c-Mpl activator stimulates human megakaryopoiesis and thrombopoiesis. Blood. 2006;107:4300-4307.
26. Kaushansky K, Broudy VC, Lin N, et al. Thrombopoietin, the Mpl ligand, is essential for full megakaryocyte development. Proc Natl Acad Sci U S A. 1995;92:3234-3238.
27. Gurney AL, Carver-Moore K, de Sauvage FJ, Moore MW. Thrombocytopenia in c-mpl-deficient mice. Science. 1994;265:1445-1447.
28. Li J, Yang C, Xia Y, et al. Thrombocytopenia caused by the development of antibodies to thrombopoietin. Blood. 2001;98:3241-3248.
29. Basser RL, O'Flaherty E, Green M, Edmonds M, Nichol J, Menchaca DM. Development of pancytopenia with neutralizing antibodies to thrombopoietin after multicycle chemotherapy supported by megakaryocyte growth and development factor. Blood. 2002;99:2599-2602.
30. Kuter DJ. New thrombopoietic growth factors. Blood. 2007;109:4607-4616.
31. Bussel JB, Kuter DJ, Phil D, et al. AMG 531, a thrombopoiesis stimulating protein, for chronic ITP. N Engl J Med. 2006;355:1672-1681.
32. Bussel J, Cheng G, Saleh M, et al. Analysis of bleeding in patients with immune thrombocytopenic purpura (ITP): a randomized, double-blind, placebo-controlled trial of eltrombopag, an oral platelet growth factor [abstract]. Blood. 2006;108:475.

33. Desjardins RE, Tempel DL, Lucker R, Kuter DJ. Single and multiple oral doses of AKR-501 (YM477) increase the platelet count in healthy volunteers [abstract]. Blood. 2006;108:477.
34. Choi ES, Nichol JL, Hokom MM, Hornkohl AC, Hunt P. Platelets generated in vitro from proplatelet-displaying human megakaryocytes are functional. Blood. 1995;85:402-413.
35. Ault KA, Knowles C. In vivo biotinylation demonstrates that reticulated platelets are the youngest platelets in circulation. Exp Hematol. 1995;23: 996-1001.
36. Guideline for animal experimentation [in Japanese]. Exp Anim. 1987;36:285-288.
37. Suzuki H, Tanoue K, Yamazaki H. Endocytosis by platelets during cationized ferritin-induced aggregation. Cell Tissue Res. 1985;240:513-517.
38. Shivdasani RA, Fujuwara Y, McDevitt MA, Orkin SH. A lineage-selective knockout establishes the critical role of transcription factor GATA-1 in megakaryocyte growth and platelet development. EMBO J. 1997;16:3965-3974.
39. Shavit JA, Motohashi H, Onodera K, Akasaka J, Yamamoto M, Engel JD. Impaired megakaryopoiesis and behavioral defects in mafG-null mutant mice. Genes Dev. 1998;12:2164-2174.
40. Shivdasani RA, Rosenblatt MF, Zucker-Franklin D, et al. Transcription factor NF-E2 is required for platelet formation independent of the actions of thrombopoietin/MGDF in megakaryocyte development. Cell. 1995;81:695-704.
41. Cramer EM, Debili N, Martin JF, et al. Uncoordinated expression of fibrinogen compared with thrombospondin and von Willebrand factor in maturing human megakaryocytes. Blood. 1989;73: 1123-1129.
42. Muntean AG, Pang L, Poncz M, Dowdy SF, Blobel GA, Crispino JD. Cyclin D-Cdk4 is regulated by GATA-1 and required for megakaryocyte growth and polyploidization. Blood. 2007;109: 5199-5207.
43. Igarashi K, Kataoka K, Itoh K, Hayashi N, Nishizawa M, Yamamoto M. Regulation of transcription by dimerization of erythroid factor NF-E2 p45 with small Maf proteins. Nature. 1994;367: 568-572.
44. Onodera K, Shavit JA, Motohashi H, Yamamoto M, Engel JD. Perinatal synthetic lethality and hematopoietic defects in compound mafG: mafK mutant mice. EMBO J. 2000;19:1335-1345.
45. Ishida N, Oritani K, Shiraga M, et al. Differential effects of a novel IFN-zeta/limitin and IFN-alpha on signals for Daxx induction and Crk phosphorylation that couple with growth control of megakaryocytes. Exp Hematol. 2005;33:495-503.
46. Platanias LC, Uddin S, Bruno E, et al. CrkL and CrkII participate in the generation of the growth inhibitory effects of interferons on primary hematopoietic progenitors. Exp Hematol. 1999;27: 1315-1321.
47. Gongora R, Stephan RP, Zhang Z, Cooper MD. An essential role for Daxx in the inhibition of B lymphopoiesis by type I interferons. Immunity. 2001;14:727-737.

STEM CELLS®

TISSUE-SPECIFIC STEM CELLS

Quiescent Human Hematopoietic Stem Cells in the Bone Marrow Niches Organize the Hierarchical Structure of Hematopoiesis

TAKASHI YAHATA,[a,b,c] YUKARI MUGURUMA,[a] SHIZU YUMINO,[a] YIN SHENG,[a] TOMOKO UNO,[a] HIDEYUKI MATSUZAWA,[a] MAMORU ITO,[d] SHUNICHI KATO,[a,c] TOMOMITSU HOTTA,[a,b] KIYOSHI ANDO[a,b]

[a]Division of Hematopoiesis, Research Center for Regenerative Medicine; [b]Department of Hematology; [c]Department of Cell Transplantation and Regenerative Medicine; Tokai University School of Medicine, Kanagawa, Japan; [d]Central Institute for Experimental Animals, Kawasaki, Japan

Key Words. Cell cycle • Clonal assays • Hematopoietic stem cell transplantation • Long-term repopulation • Mesenchymal stem cells • Stem cell-microenvironment interactions • Human hematopoietic stem cells • Severe combined immunodeficient repopulating cell

ABSTRACT

Hematopoiesis is a dynamic and strictly regulated process orchestrated by self-renewing hematopoietic stem cells (HSCs) and the supporting microenvironment. However, the exact mechanisms by which individual human HSCs sustain hematopoietic homeostasis remain to be clarified. To understand how the long-term repopulating cell (LTRC) activity of individual human HSCs and the hematopoietic hierarchy are maintained in the bone marrow (BM) microenvironment, we traced the repopulating dynamics of individual human HSC clones using viral integration site analysis. Our study presents several lines of evidence regarding the in vivo dynamics of human hematopoiesis. First, human LTRCs existed in a rare population of CD34 CD38 cells that localized to the stem cell niches and maintained their stem cell activities while being in a quiescent state. Second, clonally distinct LTRCs controlled hematopoietic homeostasis and created a stem cell pool hierarchy by asymmetric self-renewal division that produced lineage-restricted short-term repopulating cells and long-lasting LTRCs. Third, we demonstrated that quiescent LTRC clones expanded remarkably to reconstitute the hematopoiesis of the secondary recipient. Finally, we further demonstrated that human mesenchymal stem cells differentiated into key components of the niche and maintained LTRC activity by closely interacting with quiescent human LTRCs, resulting in more LTRCs. Taken together, this study provides a novel insight into repopulation dynamics, turnover, hierarchical structure, and the cell cycle status of human HSCs in the recipient BM microenvironment. STEM CELLS *2008;26:3228–3236*

Disclosure of potential conflicts of interest is found at the end of this article.

INTRODUCTION

One of the essential features of hematopoietic stem cells (HSCs) is their ability to remain in a quiescent state to maintain long-term repopulating activity [1]. Regulatory mechanisms that govern this quiescent state are crucial for organizing the hierarchical structure of hematopoiesis and are also of critical biological importance in preventing premature HSC exhaustion under conditions of hematopoietic stress. Several murine studies have demonstrated that interactions between HSCs and stem cell niches, specialized bone marrow (BM) microenvironments created by supporting cells, via receptor-ligand interactions and cell-adhesion molecules expressed in both cell types play central roles in regulating stem cell properties [2]. At present, at least two distinct niches have been identified in the endosteal areas of BM: the osteoblastic niche and the vascular niche [3–5]. However, it remains unclear whether these principles of the niche-HSC regulatory system, extrapolated from murine studies, could apply to human situations.

The severe combined immunodeficient (SCID) mouse-repopulating cell (SRC) assay is considered to be the most reliable research tool for in vivo analysis of the biological processes of human hematopoiesis [6]. In this assay system, SRCs, defined by their ability to reconstitute human hematopoiesis in immunodeficient mice, can be classified into several subtypes on the basis of the lineage restriction of their progenies and the timing of their appearance after transplantation. Although long-term repopulating cell (LTRC) activities with lymphomyeloid potential are mostly restricted to the CD34 $CD38^{neg}$ population, the CD34 CD38 population exhibits only short-term repopulating cell (STRC) activities [7–9]. STRCs are further subdivided into myeloid-restricted STRCs (STRC-Ms) and lymphomyeloid STRCs (STRC-MLs) [10]. The hierarchical relationships of each SRC pop-

Author contributions: T.Y.: conception and design, collection and assembly of data, data analysis and interpretation, and manuscript writing; Y.M.: collection and assembly of data, data analysis and interpretation, and manuscript writing; S.Y., Y.S., T.U., and H.M.: collection of data; M.I., S.K.: provision of study material; T.H. and K.A.: conception and design, financial support, and final approval of manuscript.

Correspondence: Kiyoshi Ando, M.D., Ph.D., Division of Hematopoiesis, Research Center for Regenerative Medicine and Department of Hematology, Tokai University School of Medicine, 143 Shimokasuya, Isehara, Kanagawa 259-1193, Japan. Telephone: 81-463-93-1121; Fax: 81-463-92-4511; e-mail: andok@keyaki.cc.u-tokai.ac.jp Received June 11, 2008; accepted for publication September 3, 2008; first published online in STEM CELLS *EXPRESS* September 11, 2008. 1066-5099/2008/$30.00/0 doi: 10.1634/stemcells.2008-0552

ulation and the precise characteristics regarding functions of individual human HSCs remain elusive.

Clonal analysis of the unique proviral integration sites is a powerful approach to identify and trace the activity of individual SRCs for comprehensive understanding of the properties of individual HSCs [11]. Random and permanent integration of virus vectors into the host cell genome makes the vector-genomic DNA junction a unique marker by which to identify the originally transduced cells and their progenies. By combining lineage-cell sorting and a linear amplification-mediated (LAM)-polymerase chain reaction (PCR) technique that verifies individual proviral integration into the human genome by direct sequence, we have developed a strategy by which to examine the multipotency of a single human HSC from two angles [12]. First, clonal analysis of each lineage cell proves the presence of the repopulating cell, which is the ancestor of the currently analyzed lineage cell (retrospective identification). Second, the stem cell phenotype and the capacity of individual SRC clones at the time of analysis distinguish self-renewing clones and differentiating clones (current status identification). Using this approach, we have recently documented heterogeneity among individual SRC clones regarding their stem cell activity, differentiation potential, and clonal longevity within the stem cell pool [12].

In this study, we investigated the in vivo repopulating dynamics of 228 sequence-verified individual SRC clones with respect to differentiation potential, self-renewal capacity, and cell cycle status in the niche. We successfully identified human LTRCs that were responsible for lifelong hematopoiesis in the BM microenvironment. Those human LTRCs localized to and interacted with the key components of the stem cell niche in a quiescent state. Once activated, they divided into LTRCs and STRCs by asymmetric self-renewal division, ultimately creating a hierarchical hematopoietic structure.

MATERIALS AND METHODS

Collection and Fractionation of Cord Blood CD34 Cells

Cord blood (CB) samples were obtained from full-term deliveries according to the institutional guidelines approved by the Tokai University Committee on Clinical Investigation. CD34 cell fractions were prepared using the CD34 Progenitor Cell Isolation Kit (Miltenyi Biotec, Sunnyvale, CA, http://www.miltenyibiotec.com). Pooled CD34 -enriched cells from multiple donors were stained with allophycocyanin (APC)-conjugated anti-lineage-specific antigens CD3 (UCHT1), CD41 (P2), glycophorin A (11E4B-7-6) (all from Coulter/Immunotech, Marseille, France), CD14 (MfP9), CD19 (SJ25C1), and CD56 (NCAM16.2) (all from BD Biosciences, San Jose, CA, http://www.bdbiosciences.com) and with phycoerythrin (PE)-conjugated anti-CD38 (HB7; BD Biosciences) and fluorescein isothiocyanate (FITC)-conjugated anti-CD34 (581; Beckman Coulter, Fullerton, CA, http://www.beckmancoulter.com) monoclonal antibodies. Cells were gated on lineage marker-negative and/or low-expression region, and Lin ^{low}CD34 cells were fractionated according to their CD38 expression levels using the FACSVantage flow cytometer (BD Biosciences). To eliminate the contamination of each subpopulation, we performed two consecutive rounds of cell sorting to ensure more than 99% cell purity.

Lentivirus Infection

Fractionated CD34 cells were plated on fibronectin CH-296 fragment (Takara Shuzo, Shiga, Japan, http://www.takara-bio.co.jp) and incubated with highly concentrated viral supernatant at a multiplicity of infection of 50 in serum-free StemPro-34 medium (Invitrogen, Carlsbad, CA, http://www.invitrogen.com) containing the following cytokines for 16 hours: recombinant human thrombopoietin (50 ng/ml; kindly donated by Kirin Brewery Co., Tokyo, http://www.kirin.co.jp/english), stem cell factor (50 ng/ml; donated by Kirin Brewery), and Flk-2/Flt-3 ligand (50 ng/ml; R&D Systems Inc., Minneapolis, http://www.rndsystems.com). The infection efficiency was 72.4% 8.5%.

Human Hematopoietic Repopulation

NOD/Shi-scid, IL-2R c^{null} (NOG) mice were obtained from the Central Institute for Experimental Animals (Kawasaki, Japan) and maintained in the animal facility of the Tokai University School of Medicine in microisolator cages; the animals were fed with autoclaved food and water. This strain exhibits a high engraftment rate of human hematopoietic cells than other existing strains such as NOD/SCID and NOD/SCID/ 2m^{null}, allowing the reconstitution capacity and lymphomyeloid differentiation of human repopulating stem cells to be assessed [13, 14]. Nine- to 20-week-old NOG mice were irradiated with 250 cGy of x-rays. The following day, transduced cells were injected into the retro-orbital plexus of the NOG mice. At the indicated times after transplantation, the mice were humanely killed, and BM cells, splenocytes, and thymocytes were harvested. Human hematopoietic cells were distinguished from mouse cells by the expression of human CD45. Enhanced green fluorescent protein (EGFP)-expressing CD45 human hematopoietic cells were further classified into human stem/progenitor (CD34), myeloid (CD33), B-lymphoid (CD19), and T-lymphoid (CD3 or CD4 /CD8) subpopulations and were sorted using a FACSVantage Diva option (BD Biosciences). Sorted populations had purities of more than 99%. All experiments were approved by the animal care committee of Tokai University.

Secondary Transplantation

BM cells were obtained from mice transplanted with CD34 CD38^{neg} cells at 18 weeks after transplantation, and CD34 cells were isolated by cell sorting. Purified CD34 cells of the primary recipients were divided in half and injected intravenously into two sublethally irradiated secondary NOG recipients (1.5 10^6 cells per recipient). One recipient was sacrificed at 3 weeks and the other at 18 weeks after transplantation. BM cells and thymocytes were collected from each secondary recipient and used for flow cytometric analysis and lineage cell sorting as described earlier.

Integration Site Analysis of Lentivirally Marked SRCs

Genomic DNA isolation and LAM-PCR were carried out as described previously [12]. The proviral integration sites of CD33 cells were sequenced, and the sequences were examined for alignment to the human genome using NCBI BlastN (http://www.ncbi.nlm.nih.gov/blast). The verified genomic sequence information of these CD33 cell integration sites was used to design new primers (all primer sequences used in this study are listed in supplemental online Tables 1 and 2). PCR was performed on each LAM-PCR product using the unique genomic flanking primers.

Estimation of Clone Size by Real-Time Quantitative PCR

The relative clone size of individual LTRC clones that was detected in the CD34 cells of primary and secondary recipients was examined as described previously [12]. For real-time quantitative PCR, each target DNA was amplified on the same plate, with -globin as the reference, using the QuantiTect SYBR Green PCR Master Mix (Qiagen, Hilden, Germany, http://www1.qiagen.com) and the ABI Prism 7700 Sequence Detection System (Applied Biosystems, Foster City, CA, http://www.appliedbiosystems.com). The relative clone amounts and range were determined in reference to -globin. A comparative threshold cycle (C_T) was used to determine the proportion of CD34 clones in paired recipients. For each sample, the clone C_T value was normalized using the formula C_T $C_{T\ clone}$ $C_{T\ -globin}$. To determine relative clone size, the following formula was used: C_T $C_{T\ clone}$ in CD34 cells of the primary recipient $C_{T\ clone}$ in CD34 cells of the secondary

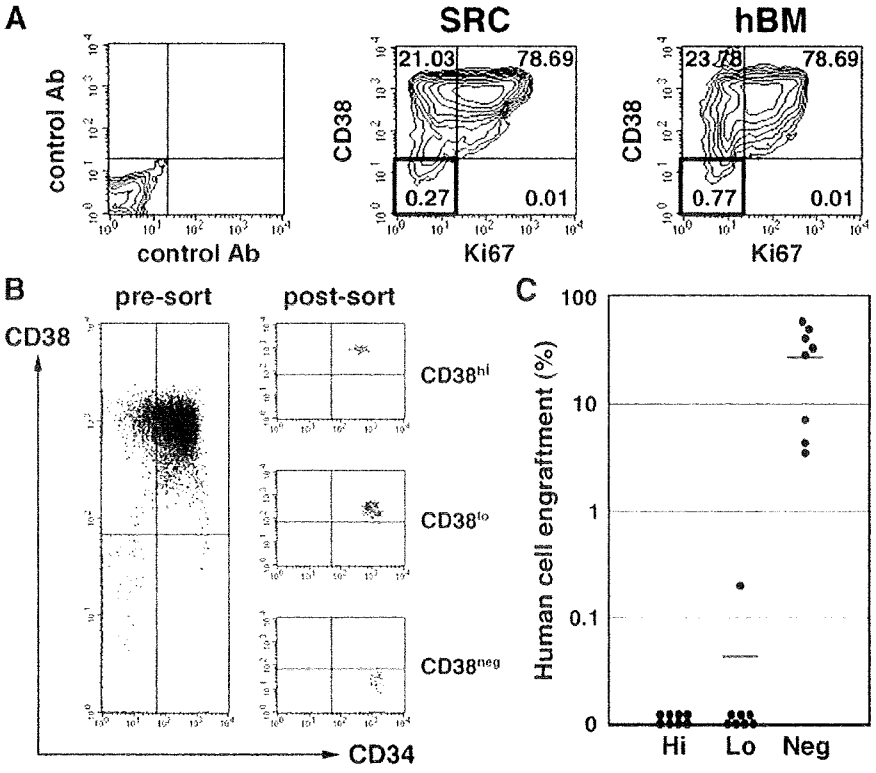

Figure 1. Cell cycle status and stem cell activity of CD34 cells. **(A):** Bone marrow (BM) CD34 cells were analyzed for their expression of CD38 and Ki-67 by flow cytometry. Representative fluorescence-activated cell sorting profiles of isotype control; CD34 cells in the NOD/Shi-scid, IL-2R c^{null} (NOG) recipient BM; and freshly isolated hBM CD34 cells from five independent experiments are shown. The relative frequencies of each population are indicated. **(B):** Representative sorting profiles of CD34 cells obtained from primary recipient BM. Fractionated CD34 cells were transplanted into secondary NOG hosts (CD34 $CD38^{neg}$, 1–7 10^4 cells; CD34 $CD38^{lo}$, 1–3.5 10^5 cells; CD34 $CD38^{hi}$, 5–8 10^5 cells). **(C):** Secondary recipient BM cells were analyzed for the expression of human CD45. Each symbol represents one mouse, and horizontal bars indicate the average engraftment level in three independent experiments. Abbreviations: Ab, antibody; hBM, human bone marrow; Hi, high; Lo, low; Neg, negative; SRC, severe combined immunodeficient mouse-repopulating cell.

recipient. The value was calculated by the expression 2 ^{C_T}. Each reaction was performed at least in triplicate.

Cell Cycle Analysis

CD34 BM cells were stained with PE-conjugated anti-CD38 and APC-conjugated anti-CD34 antibodies. The cells were then fixed and permeabilized using a Cell Permeabilization Kit (BD Biosciences) and stained with FITC-conjugated anti-Ki-67 antibody (BD Biosciences). Fluorescence-activated cell sorting analysis was performed on a FACSCalibur using CELLQuest software (BD Biosciences).

Histological Analysis of BM Microenvironment

Tissue processing and immunofluorescent staining were performed as described previously [15]. For in situ examination of transplanted nonhematopoietic human cells, genetically EGFP-marked human mesenchymal stem cells (MSCs) were transplanted directly into the right tibias of NOG mice. The following antibodies were used for tissue immunostaining: anti-human CD34 (My10; BD Biosciences), anti-human CD38 (HI12; BD Biosciences), anti-human CD31 (TECHNE, Minneapolis, http://www.techne-corp.com), anti-human SDF-1 (Santa Cruz Biotechnology Inc., Santa Cruz, CA, http://www.scbt.com), and anti-proliferating cell nuclear antigen (anti-PCNA; Abcam, Cambridge, U.K., http://www.abcam.com). Immunofluorescent-stained slides were examined, and images were captured using an LSM510 META confocal microscope (Carl Zeiss, Jena, Germany, http://www.zeiss.com). Images were processed by Adobe Photoshop 7.0 (Adobe Systems Inc., San Jose, CA, http://www.adobe.com).

Statistical Analysis

Data are represented as mean SD. p values .05 were considered to be significant.

RESULTS

Only Quiescent CD34 $CD38^{neg}$ Cells in the Recipient Sustain Long-Term Hematopoiesis

To investigate the characteristics of human LTRCs in the recipient BM, we transplanted CB CD34 $CD38^{neg}$ cells into sublethally irradiated NOG mice. Eighteen weeks after transplantation, we examined the cell cycle status and repopulating ability of engrafted CD34 cells in recipient BM. $CD38^{neg}$ cells accounted for a very small population of CD34 cells in the BM of transplanted mice (1.33% 1.18%; n 7). The expression of Ki-67, a nuclear protein expressed during all active parts of the cell cycle in proliferating cells, was examined to evaluate the cell cycle status of CD34 cells in the BM of transplanted mice. Although a majority of CD34 CD38 cells expressed Ki-67, less than 0.1% of CD34 $CD38^{neg}$ cells were positive for Ki-67 (Fig. 1A), confirming that CD34 $CD38^{neg}$ cells in the recipient BM were indeed dormant. Interestingly, the cell surface phenotype, high levels of CD38 expression in the majority of CD34 cells, and the cell cycle status of CD34 cells in the NOG mice closely resembled those of human BM-derived CD34 cells (Fig. 1A), suggesting that the human BM microenvironment of NOG mouse can substitute, at least in part, for the function of a human BM microenvironment.

To examine the LTRC activity of CD34 cells in recipient BM, we separated CD34 cells into $CD38^{neg}$, $CD38^{lo}$, and $CD38^{hi}$ fractions and transplanted these fractions into secondary NOG hosts (Fig. 1B). Secondary transplantable LTRCs were found almost exclusively in the extremely rare fraction of CD34 $CD38^{neg}$ cells (Fig. 1C). These cells were able to display multilineage engraftment in secondary recipients (supplemental online Fig. 1). Our results revealed that CD34 $CD38^{neg}$ cells in recipient BM stayed in the quiescent state and that only these

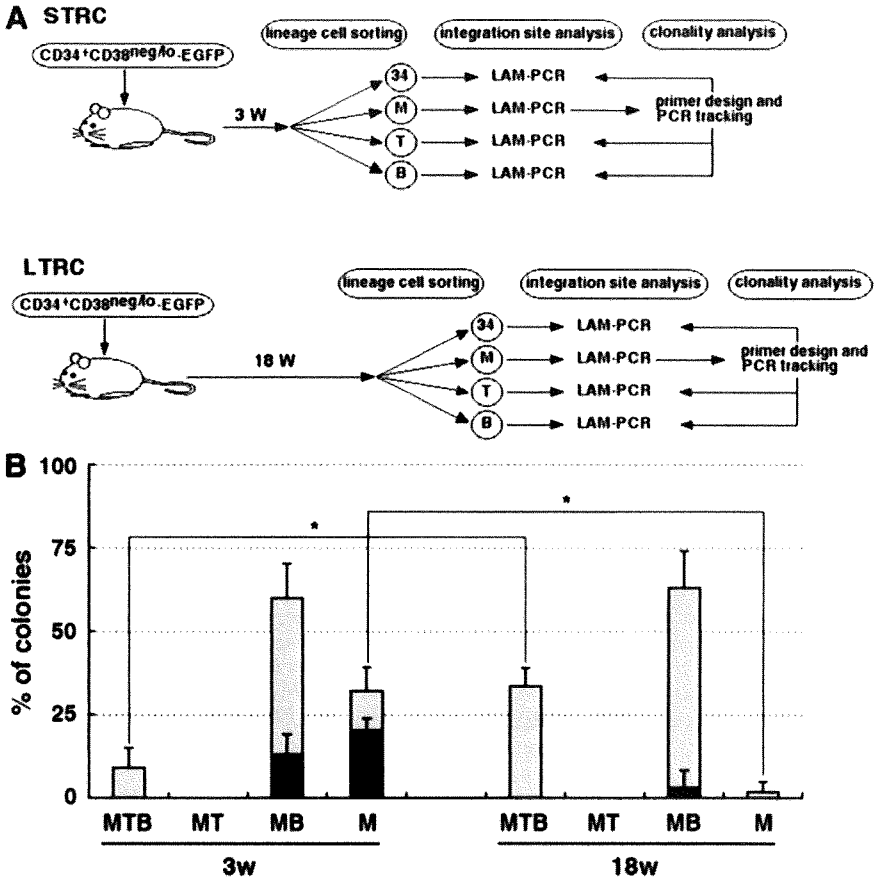

Figure 2. Differentiation ability and self-renewal capacity of individual severe combined immunodeficient mouse-repopulating cell clones. (**A**): Study design for clonal analysis of STRC and LTRC activity. (**B**): Relative frequencies of each clone type. Gray areas in each bar represent the clones detected in CD34 cells, and black areas represent the clones not detected in CD34 cells. A total of 116 clones were analyzed (supplemental online Table 1). Mean SD of four independent experiments are shown. , p .01. Abbreviations: 34, CD34 stem/progenitor cells; B, CD19 B-lymphoid lineage cells; EGFP, enhanced green fluorescent protein; LAM, linear amplification-mediated; lo, low; LTRC, long-term repopulating cell; M, CD33 myeloid lineage cells; neg, negative; PCR, polymerase chain reaction; STRC, short-term repopulating cell; T, CD3 (spleen) or CD4/CD8 DP (thymus) T-lymphoid lineage cells; W, weeks.

cells were able to continuously reconstitute hematopoiesis in vivo.

Repopulation Dynamics of Individual SRC Clones During Human Hematopoietic Reconstitution Originated from CD34 $CD38^{neg}$ Cells

Next, we dissected out the repopulation dynamics of SRCs derived from the quiescent subpopulations of CD34 $CD38^{neg}$ cells. Following transplantation, NOG recipient mice were sacrificed at several time points, and the engraftment and development of human hematopoietic cells were analyzed. Mice that received CD34 $CD38^{neg}$ cells exhibited high levels of CD45 human hematopoietic cell engraftment at 3 weeks after transplantation (the early phase of repopulation) (supplemental online Fig. 2A). The recipients continued to display high levels of human hematopoietic cell (CD45) and stem/progenitor cell (CD34) repopulation between 9 and 18 weeks (the later phase of repopulation). As expected, the human hematopoietic graft in NOG mice consisted mainly of CD33 myeloid lineage cells at 3 weeks after transplantation, but CD19 B-lymphoid cells outgrew after 9 weeks (supplemental online Fig. 2B).

To clarify the specific stem cell activity of individual SRCs originating from quiescent CD34 $CD38^{neg}$ cells that contribute to various stages of hematopoietic reconstitution, we examined the functional aspects of individual SRC clones using LAM-PCR-based viral integration site analysis (Fig. 2A). Each NOG mouse that received EGFP-transduced CD34 $CD38^{neg}$ population was analyzed at two time points. At each time point, EGFP-expressing human hematopoietic lineage cells were sorted, and the fate of individual SRC clones was examined by clone-tracking analysis. Using primers that were designed on the basis of the genomic sequence information of the CD33 myeloid cell integration site, we traced distribution of each clone among phenotypically distinct populations: CD34 stem/progenitor, T-lymphoid, and B-lymphoid cells (all primer sequences are listed in supplemental online Table 1). Three different clone types were observed at each time point: a multipotent type (MTB), in which insertion sites originally detected in CD33 myeloid cells were also detected in T- and B-lymphoid cell populations; a unipotent progenitor containing exclusively myeloid cells; and a bipotent M/B progenitor. We found that the early phase of hematopoietic reconstitution was mostly attributed to myeloid-restricted clones (Fig. 2B; p .01 compared with later phase of reconstitution). On the other hand, the majority of SRC clones found in the later phase of hematopoiesis were of the multilineage cell-producing type (Fig. 2B; p .01).

We previously reported that the presence or the absence of a common integration site in CD34 stem cell populations indicated the current status of individual SRC clones in terms of their stem cell function [12]. The three clone types were further examined to determine whether they stayed in the CD34 stem cell pool (Fig. 2B). Consistent with our previous observations, the proportion of clones that stayed in the CD34 cell population decreased as the differentiation potential of clones restricted to bipotency or unipotency at 3 weeks, suggesting that initial myeloid-producing STRCs were rapidly exhausted from the CD34 stem cell pool. At 18 weeks, the vast majority of clones (95%) stayed in the CD34 stem cell pool, suggesting the self-replication of virally transduced SRC clones that have the ability to produce both lymphoid and myeloid lineages within the stem cell pool.

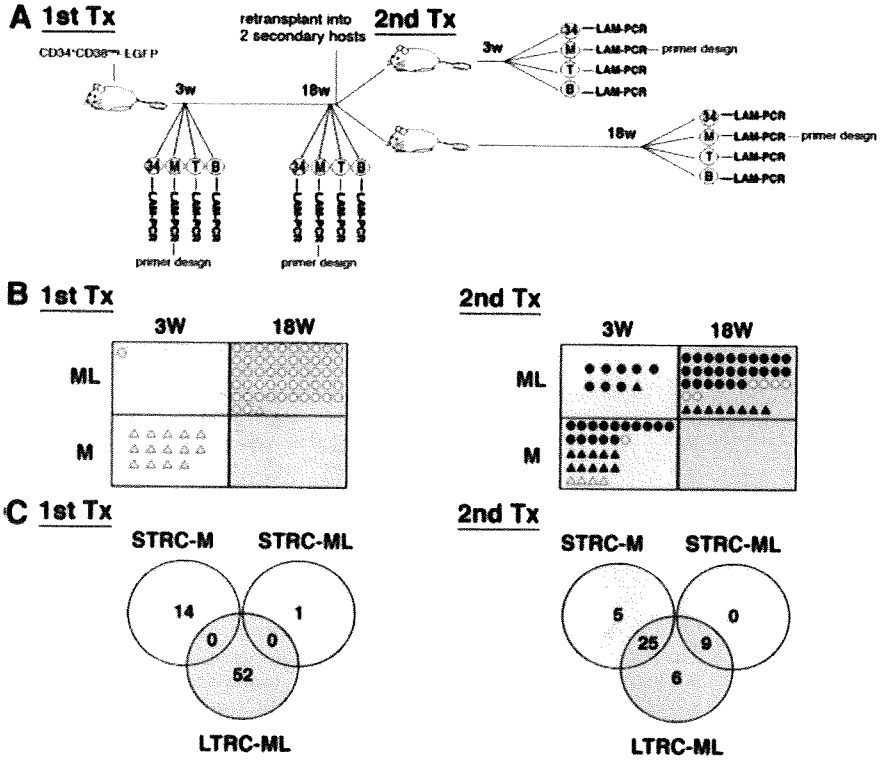

Figure 3. Sequential analysis of individual severe combined immunodeficient mouse-repopulating cell (SRC) clones derived from CD34 CD38^{neg} population. **(A):** Study design for sequential analysis of individual SRC clones. Lineage-specified cells were separated at the indicated time points, and clone-tracking analysis was performed to examine the presence and persistence of specific clones. **(B):** Summary of the sequential clone-tracking analysis from three independent experiments. A total of 112 clones were analyzed (supplemental online Table 2). Open symbols: clones detected at one time point only. Filled symbols: clones simultaneously detected at two time points. Circles: clones detected in the CD34 stem cell pool. Triangles: clones not detected in the CD34 stem cell pool. **(C):** Cumulative number of different types of clones. Numbers in overlapping circles represent clones present at both time points. Abbreviations: B, CD19 B-lymphoid lineage cells; LAM, linear amplification-mediated; LTRC, long-term repopulating cell; M, CD33 myeloid lineage cells; ML, multilineage; PCR, polymerase chain reaction; STRC, short-term repopulating cell; T, CD3 (spleen) or CD4/CD8 DP (thymus) T-lymphoid lineage cells; TX, transplantation; w, weeks.

Sequential SRC Clone-Tracking Analysis Revealed that the Quiescent CD34 CD38^{neg} Cells Constitute the Hierarchical Organization of Human Hematopoiesis

In the recipients of CD34 CD38^{neg} cells, the early phase of repopulation was dominated by myeloid-restricted clones (M-clones), as opposed to the later phase, in which the majority of repopulating clones were multilineage type clones (ML-clones) (Fig. 2B). At this point, it is not clear whether the identical clones produced different types of cells depending on the reconstitution phase or independent clones were responsible for either the early or later phase of repopulation. To find out the origin of repopulating clones in the early and later phases, we performed integration site analysis on individual clones recovered from both phases of the same CD34 CD38^{neg} cell recipient (Fig. 3A, left part; all primer sequences are listed in supplemental online Table 2). At 3 weeks after transplantation, BM cells were aspirated from the tibia of each recipient, and at 18 weeks recipients were sacrificed and BM cells were collected from four long bones. At each time point, EGFP-expressing human hematopoietic lineage cells were sorted for integration site analysis using LAM-PCR. Each proviral integration site serves as a unique marker by which to identify individual clones. When the identical proviral integration site was recognized at different time points, it was regarded as the persistence of the same clone. In that way, we were able to examine the fate of individual SRC clones in the same recipient at different time points. As reported earlier in this study (Fig. 2B), transient M-clones were responsible for the early phase of hematopoietic reconstitution, and self-replicating ML-clones were responsible for the late phase. Interestingly, the transient M-clones detected at the early phase and self-replicating ML-clones were distinctly different (Fig. 3B, 3C, left), indicating that the CD34 CD38^{neg} population, which is highly enriched for human LTRCs, is composed of distinct clonal subsets that are heterogeneous in repopulating kinetics, lineage cell-producing ability, and self-renewal capacity.

To further examine clonal differences in the repopulating cells, we performed clone-tracking analysis on paired secondary transplanted mice. CD34 cells recovered from primary recipients at 18 weeks of transplantation were subsequently transplanted into two secondary recipients, one of which was sacrificed at 3 weeks and the other at 18 weeks after secondary transplantation (Fig. 3A, right). Most of the clones (26 of 38; 68.4%) found in the primary recipients did not engraft in the secondary recipient, suggesting that the repopulating potential of most clones deteriorates during long-term reconstitution in the primary recipient. In contrast, all clones detected in paired secondary recipients had originated from the primary LTRC clones. To our interest, in all the clones found in the secondary recipient pair (a total of 45), there was a significant overlap between STRC and LTRC (34 of 45; 75.6%) (Fig. 3B, 3C, right), which is in contrast to the earlier observation in the primary recipient. This indicates that LTRCs produce both STRCs and LTRCs by asymmetric self-renewal division. It is important to note that although all the STRC-ML clones (9 of 9) demonstrated LTRC activity, some of the STRC-M clones (5 of 30; 16.7%) showed only a transient engraftment, indicating that STRC-M tends to have a more restricted potential than STRC-ML (Fig. 3B, 3C, right). We also identified a small proportion of clones (6 of 45; 13.3%) that were uniquely found in the later phase of secondary repopulation, suggesting the existence of quiescent LTRCs that are reactivated only at the later phase. Taken together, our findings constitute clonal evidence that self-replicating LTRCs produce widely heterogeneous SRC compartments, ultimately constituting hierarchical organization of the human HSC pool (supplemental online Fig. 3).

LTRCs with Higher Self-Renewal Capacity Are Constituted by Relatively Dormant Clones and Expanded Clonally upon Secondary Transplantation

Finally, we quantitatively compared the relative clone size of each LTRC clone that was found in the CD34 stem cell pool of both primary and secondary recipients. Interestingly, all

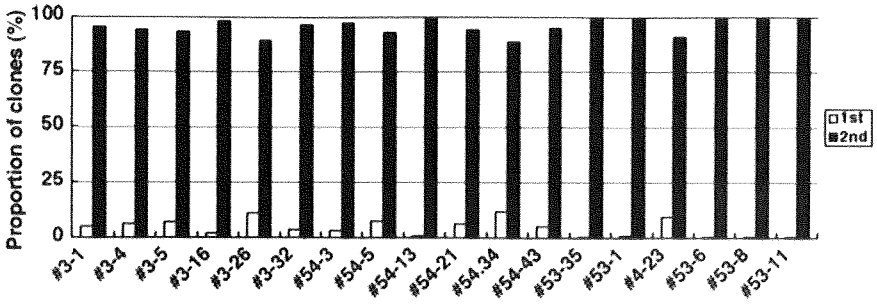

Figure 4. Relative clone size of individual long-term repopulating cell (LTRC) clones in primary and secondary recipients. The clone size of individual LTRC clones detected in CD34 cells was examined by real-time quantitative polymerase chain reaction. The relative clone sizes of each LTRC clone in primary (open bars) and secondary (filled bars) recipients are shown.

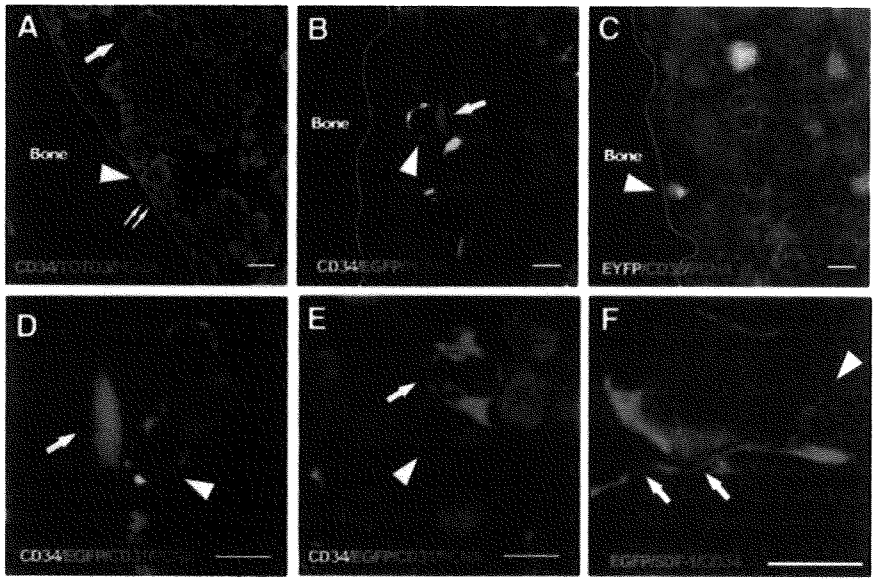

Figure 5. Quiescent human long-term repopulating cells interacting with niche components in the endosteal region. **(A):** Two human CD34 cells, a PCNA-negative (arrowhead) and a PCNA-positive (double arrows), were adjacent to each other and are attached to the endosteum. A large CD34 PCNA-positive cell was found away from endosteum (arrow). **(B):** A PCNA-negative CD34 cell (arrowhead) interacted with CD31-expressing murine endothelial cells (arrow) in the endosteal region. **(C):** The majority of human cells were positive for CD38. A $CD38^{neg}$PCNA-negative EYFP-transduced human cell was attached to the endosteum (arrowhead). **(D, E):** EGFP-marked HMRCs differentiated into fibroblastic reticular cells that associated with CD31 vascular cells. PCNA-negative quiescent CD34 cells (arrowheads) interacted with human reticular cells (arrow). **(F):** HMRCs in the vascular niche expressed SDF-1 (arrows) and interacted with a CD34 cell (arrowhead). Scale bars 10 m. Abbreviations: EGFP, enhanced green fluorescent protein; PCNA, proliferating cell nuclear antigen.

LTRC clones in the CD34 stem cell pool of the secondary recipient were much larger than they had been in the primary recipient (Fig. 4). This suggests that LTRC clones with a higher self-renewal ability are relatively inactive or proliferate slowly, but they could become activated upon secondary transplantation. We also discovered that all quiescent LTRCs were indeed capable of producing multilineage cells in the primary recipients, suggesting that stem cells are not always quiescent but can actively contribute to hematopoiesis when necessary. These results provide evidence for the clonal dynamics of repopulating clones by showing that LTRCs are quiescent at one point and are active at another point.

Quiescent LTRCs Localizes to BM Niches

Maintenance and regulation of LTRCs in vivo depends on the specific microenvironment, known as the niche. We examined the localization of quiescent human CD34 cells in the BM microenvironment of recipients. The quiescent CD34 cells were identified by the lack of PCNA expression. Most of the PCNA CD34 cells (77.8%; *n* 198 PCNA CD34 cells) were located in the endosteal region (arbitrarily defined as within 12 cells of the endosteum, as described previously [16]) and were found to be associated with bone-lining osteoblasts or endothelial cells (Fig. 5A, 5B). These niche-interacting quiescent human CD34 cells were confirmed as CD38-negative (Fig. 5C), the only cell population transplantable in secondary recipients. In line with previous mouse studies [3–5], these results revealed that human HSCs stayed in a quiescent state to maintain their LTRC activity by actively interacting with the osteoblastic and vascular niche components in the endosteal region of BM.

Mesenchymal Stem Cells Serve As Stem Cells for the Hematopoietic Microenvironment

These experiments had so far demonstrated behavior of human hematopoietic cells in the murine microenvironment. To inspect whether the principles of niche regulatory system extrapolated from murine studies could apply to the human situation, human hematopoietic reconstitution was examined in the "humanized" hematopoietic microenvironment. Previously, we established an experimental system in which a functional human microenvironment was reproduced by the intramedullary injection of human BM MSC-derived HMRCs [15]. The presence of HMRCs was shown to be important in human hematopoietic reconstitution in immunodeficient mice. We examined whether the HMRCs play roles in the maintenance of the LTRC activity in BM. EGFP-transduced human MSCs were intramedullary injected into the right tibia of irradiated NOG mice, and then CD34 cells were transplanted intravenously into each mouse. Consistent with our previous report [15], a majority of HMRCs differentiated into vasculature-associated fibroblastic reticular cells, which are known to play a pivotal role in HSC regulation [17]. In line with this notion, HMRCs expressed one of the important hematopoietic regulatory molecules, SDF-1 (Fig. 5F). Interestingly, the quiescent human CD34 cells often interacted with these EGFP human reticular cells in the endosteal region, strongly suggesting the hematopoiesis-supporting function of these cells (Fig. 5D, 5E). Much to our interest, the number of

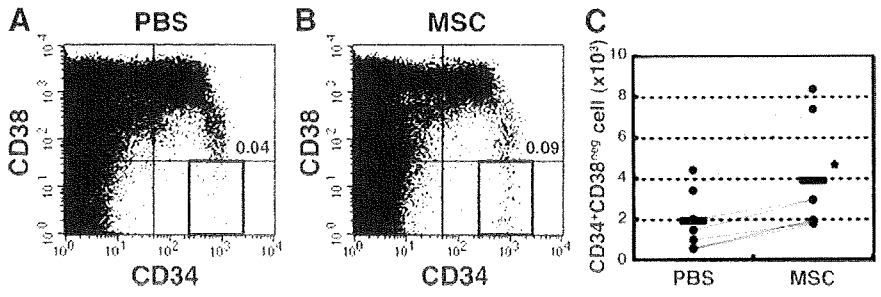

Figure 6. Effect of HMRCs on the engraftment of long-term repopulating cells. **(A):** BM cells obtained from the MSC-injected (right) or PBS-injected (left) tibia from the same mouse were examined by flow cytometry at 12 weeks after transplantation. Representative flow cytometric profiles are shown. The relative frequencies of the CD34 $CD38^{neg}$ population are indicated. **(B):** Absolute numbers of CD34 $CD38^{neg}$ cells in the MSC-injected (right) and the PBS-injected (left) tibias of mice. Each dot represents one mouse. Values obtained from the same mouse are connected with lines. , p .01 relative to the PBS-injected tibia. Abbreviations: MSC, mesenchymal stem cell; neg, negative; PBS, phosphate-buffered saline.

CD34 $CD38^{neg}$ LTRCs in the HMRC-injected tibia was higher than in the saline-injected tibia in the same recipient (Fig. 6). These results confirmed the previous mouse study and demonstrated for the first time that human reticular cells in the endosteal niches were one of the critical components of human LTRC niches.

DISCUSSION

In this study, we demonstrated that the hierarchical organization of human HSCs originated from quiescent CD34 $CD38^{neg}$ cells that resided in the endosteal region of the BM microenvironment, particularly in osteoblastic and vascular niches. Our study presented several lines of evidence that are important in understanding the in vivo dynamics of human hematopoiesis. First, human hematopoiesis was supported by functionally heterogeneous and distinct clonal subsets. Human repopulating cells with predetermined STRC activity contributed to the initial myeloid production, and those clones were rapidly exhausted from the CD34 stem cell pool and lost repopulating ability. In contrast, multilineage-producing LTRC clones remained in the CD34 stem cell pool and sustained hematopoiesis. Asymmetric division of LTRC clones produced clones with different potentials, resulting in the construction of the hierarchical organization of the human HSC pool in the BM microenvironment. Second, repopulating activity of long-lasting LTRCs fluctuated. We quantitatively demonstrated that the self-renewing LTRCs normally stayed in a quiescent state in the primary recipient and expanded clonally upon secondary transplantation. Finally, the hematopoietic microenvironment activity influenced LTRC maintenance. We demonstrated that MSCs served as stem cells for the key components of the hematopoietic microenvironment and that the number of LTRCs could be increased by manipulating microenvironments.

Stem cell quiescence is an indispensable property for the maintenance of hematopoiesis. Interaction of HSCs with their particular microenvironments, known as the stem cell niches, is critical in regulating stem cell quiescence [2]. Although it has been reported that the most primitive human hematopoietic cells, when freshly isolated [18–22], stayed predominantly in the quiescent phase, the cell cycle status and potential of transplanted human HSCs in recipient BM has not been fully examined. In this study, we successfully demonstrated that human LTRCs existed in a rare population of CD34 CD38 cells that localized to the stem cell niches and maintained their stem cell activities while remaining in a quiescent state. Furthermore, we successfully visualized interaction between BM niche cells and a rare population of dormant LTRCs that fulfilled the functional criteria of HSCs: cell cycle quiescence and multilineage engraftment in a secondary host. Combined with our previous finding that showed preferential localization of transplanted CD34 $CD38^{neg}$ cells in the endosteal area [15], the present study indicates that LTRCs protect themselves from extinguishing their stem cell activity by firmly attaching to the endosteal niches in cases of various hematopoietic stresses, as has been demonstrated in mouse studies [23, 24].

Several studies, including the present one, showed that LTRC activity was highly enriched in the CD34 $CD38^{neg}$ fraction, and the self-renewal capacity and differentiation potential of SRCs became restricted, coinciding with the appearance and increasing expression of the CD38 antigen [7–10]. Recently, unexpectedly high repopulating activity was discovered within a CD34 $CD38^{lo}$ subpopulation in direct intrafemoral transplantation experiments [25]. However, the present study demonstrated that CD34 $CD38^{lo}$ cells appeared to be more restricted in their self-renewal ability. Although we were unable to determine the reason for this discrepancy, it is possible that the high self-renewal activity of the CD34 $CD38^{lo}$ subpopulation could be grasped only by direct intrafemoral transplantation. Nevertheless, our experiment has presented the idea that the self-renewal potentials of the CD34 $CD38^{lo}$ and CD34 $CD38^{neg}$ fractions are distinctly different. Furthermore, we demonstrated for the first time that a rare population of CD34 $CD38^{neg}$ cells in the primary recipient BM niches was the only group of SRCs that could successfully reconstitute hematopoiesis in the secondary recipient.

A previous study has reported that in an event that enforces active proliferation of HSCs, such as transplantation, initial active proliferation of SRC population is markedly downregulated after a while [26]. Another study demonstrated an initial upsurge and rapid decline of STRCs in human subjects [27]. Our study showed a similar decline of STRCs. Importantly, our clone-tracking lineage analysis revealed that transient unipotent STRC repopulation was followed by the emergence of multipotent LTRCs. Those LTRCs became activated and produced self-renewing LTRCs and STRCs with limited self-renewal activity. These STRCs in the later phase served as a functional element of the hematopoietic hierarchy. Together with earlier findings, the results of our study provided experimental evidence that quiescent human LTRCs asymmetrically divide in the BM niches, producing one daughter cell that remains in a quiescent state as a "reservoir" of the stem cell pool and another daughter cell that proliferates and differentiates into CD38 cells as a "contributor" for sustaining hematopoiesis.

Several studies in mice and larger animals have concluded that long-term hematopoiesis is sustained by a limited number of self-renewing stem cells that maintain their stem cell activities by staying in a quiescent state and are activated as the occasion demands [28–32]. However, the quantitative dynamics

of individual HSC clones during a quiescent state and an active state remain unclear. In the present study, we quantitatively unveiled that self-renewing LTRC clones normally occupied very small clone size in the primary recipient but expanded remarkably (10–1,000-fold) upon secondary transplantation. Importantly, these quiescent LTRCs were capable of producing multilineage cells even in a steady state in the primary recipients, suggesting that stem cells are not always remained in a quiescent state but can actively contribute to hematopoiesis, depending on the situation.

The exact nature of the HSC niche and the mechanism of HSC regulation have remained largely unknown because of the complex structure of the niche itself and the technical difficulties of examining it. Over the past few years, however, a number of important papers have been published [3–5, 17], and we began to understand how the niche regulates HSCs, at least in mice. Unfortunately, experimental examination of human hematopoietic niches had been hampered by the lack of an appropriate model system until now. We recently established a mouse model that recapitulates a functional human hematopoietic microenvironment [15]. Intramedullary transplanted human MSCs, termed HMRCs, reconstituted functional components of hematopoietic niches. The majority of HMRCs became fibroblastic reticular cells that were often associated with the vasculature, and the rest differentiated into osteoblasts, osteocytes, and endothelial cells. These HMRCs actively interacted with primitive human HSCs to maintain secondary transplantable repopulating activity. Importantly, the HMRCs preferentially distributed to the endosteal region and expressed several niche factors, such as N-cadherin [4], SDF-1 [33–35], and fibronectin [35–37] (T.Y., Y.M., and K.A., unpublished observation). In another published study [35], we demonstrated the important in vivo roles of these niche factors, especially SDF-1, for the engraftment of human HSCs in the BM microenvironment by directly injecting antibody-treated human HSCs into the BM cavity. In the present study, quiescent HSCs interacted with HMRC-derived human reticular cells, and cotransplantation with MSCs resulted in increased engraftment of the CD34 $CD38^{neg}$ population (i.e., the LTRC compartment), emphasizing the importance of the presence of a human microenvironment in an experimental animal. Consistent with our past [15] and present findings, a recent study by Sugiyama et al. elegantly demonstrated that SDF-1-expressing fibroblastic reticular cells play a pivotal role in both osteoblastic and vascular niches at the endosteal region of the murine microenvironment [17]. Taken together, those findings and our own indicated that HMRC-derived fibroblastic reticular cells in the osteoblastic and vascular niches participate in the maintenance of LTRC activity by closely interacting with quiescent human HSCs and secreting hematopoietic-regulatory factors.

Detailed examinations of the innate properties of individual human HSCs that contribute to various phases of reconstitution is important not only to understand human hematopoietic development but also to exploit the therapeutic potential of HSCs. Clinically speaking, rapid recovery of hematopoiesis and sustainable long-term hematopoiesis in patients are primary factors for successful HSC transplantation. In other words, appropriate control of initial hematopoietic recovery and prevention of premature HSC exhaustion could remarkably improve the therapeutic outcome of clinical transplantation. The clonal analysis presented in this study enabled us to accurately evaluate in vivo properties of individual human HSCs. Our strategies may serve as indicators to assess the therapeutic effects of emerging stem cell therapies and help advance clinical transplantation medicine.

CONCLUSION

Through this study, we successfully identified human LTRCs that were responsible for lifelong hematopoiesis in the BM microenvironment. In a steady state, those quiescent human LTRCs localized to and interacted with the key components of the stem cell niche. Once activated, they divided asymmetrically into LTRCs and STRCs, ultimately creating a hierarchical hematopoietic structure. Further identification and characterization of LTRC and STRC subsets will be particularly useful in optimizing protocols for stem cell therapies. Our study also confirmed that MSCs serve as stem cells for the key components of the hematopoietic microenvironment. Therefore, it should be possible to develop MSCs into useful therapeutic tools for conditioning the hematopoietic niches.

ACKNOWLEDGMENTS

We thank members of the animal facility of Tokai University for meticulous care of the experimental animals and members of the Tokai Cord Blood Bank for assistance. We also thank members of the Research Center for Regenerative Medicine of Tokai University for helpful discussion and assistance. This work was supported in part by Grants-in-Aid for Scientific Research from the Ministry of Education, Culture, Sports, Science, and Technology of Japan and by a Research Grant on Human Genome, Tissue Engineering from The Ministry of Health, Labor, and Welfare of Japan.

DISCLOSURE OF POTENTIAL CONFLICTS OF INTEREST

The authors indicate no potential conflicts of interest.

REFERENCES

1 Cheng T, Rodrigues N, Shen H et al. Hematopoietic stem cell quiescence maintained by p21cip1/waf1. Science 2000;287:1804–1808.
2 Wilson A, Trumpp A. Bone-marrow haematopoietic-stem-cell niches. Nat Rev Immunol 2006;6:93–106.
3 Calvi LM, Adams GB, Weibrecht KW et al. Osteoblastic cells regulate the haematopoietic stem cell niche. Nature 2003;425:841–846.
4 Zhang J, Niu C, Ye L et al. Identification of the haematopoietic stem cell niche and control of the niche size. Nature 2003;425:836–841.
5 Kiel MJ, Yilmaz OH, Iwashita T et al. SLAM family receptors distinguish hematopoietic stem and progenitor cells and reveal endothelial niches for stem cells. Cell 2005;121:1109–1121.
6 Shultz LD, Ishikawa F, Greiner DL. Humanized mice in translational biomedical research. Nat Rev Immunol 2007;7:118–130.
7 Bhatia M, Wang JC, Kapp U et al. Purification of primitive human hematopoietic cells capable of repopulating immune-deficient mice. Proc Natl Acad Sci U S A 1997;94:5320–5325.
8 Hogan CJ, Shpall EJ, Keller G. Differential long-term and multilineage engraftment potential from subfractions of human CD34 cord blood cells transplanted into NOD/SCID mice. Proc Natl Acad Sci U S A 2002;99:413–418.
9 Kerre TC, De Smet G, De Smedt M et al. Both CD34 38 and CD34 38- cells home specifically to the bone marrow of NOD/LtSZ scid/scid mice but show different kinetics in expansion. J Immunol 2001;167:3692–3698.
10 Glimm H, Eisterer W, Lee K et al. Previously undetected human hematopoietic cell populations with short-term repopulating activity selec-

tively engraft NOD/SCID-beta2 microglobulin-null mice. J Clin Invest 2001;107:199–206.
11 Guenechea G, Gan OI, Dorrell C et al. Distinct classes of human stem cells that differ in proliferative and self-renewal potential. Nat Immunol 2001;2:75–82.
12 Yahata T, Yumino S, Seng Y et al. Clonal analysis of thymus-repopulating cells presents direct evidence for self-renewal division of human hematopoietic stem cells. Blood 2006;108:2446–2454.
13 Yahata T, Ando K, Nakamura Y et al. Functional human T lymphocyte development from cord blood CD34 cells in nonobese diabetic/Shi-scid, IL-2 Receptor Gamma Null Mice J Immunol 2002;169:204–209.
14 Ito M, Hiramatsu H, Kobayashi K et al. NOD/SCID/gamma(c)(null) mouse: An excellent recipient mouse model for engraftment of human cells. Blood 2002;100:3175–3182.
15 Muguruma Y, Yahata T, Miyatake H et al. Reconstitution of the functional human hematopoietic microenvironment derived from human mesenchymal stem cells in the murine bone marrow compartment. Blood 2006;107:1878–1887.
16 Nilsson SK, Johnston HM, Coverdale JA. Spatial localization of transplanted hemopoietic stem cells: Inferences for the localization of stem cell niches. Blood 2001;97:2293–2299.
17 Sugiyama T, Kohara H, Noda M et al. Maintenance of the hematopoietic stem cell pool by CXCL12-CXCR4 chemokine signaling in bone marrow stromal cell niches. Immunity 2006;25:977–988.
18 Jordan CT, Yamasaki G, Minamoto D. High-resolution cell cycle analysis of defined phenotypic subsets within primitive human hematopoietic cell populations. Exp Hematol 1996;24:1347–1355.
19 Hao QL, Shah AJ, Thiemann FT et al. A functional comparison of CD34 CD38- cells in cord blood and bone marrow. Blood 1995;86:3745–3753.
20 Gothot A, van der Loo JC, Clapp DW et al. Cell cycle-related changes in repopulating capacity of human mobilized peripheral blood CD34( ) cells in non-obese diabetic/severe combined immune-deficient mice. Blood 1998;92:2641–2649.
21 Summers YJ, Heyworth CM, de Wynter EA et al. Cord blood G(0) CD34 cells have a thousand-fold higher capacity for generating progenitors in vitro than G(1) CD34 cells. STEM CELLS 2001;19:505–513.
22 Byk T, Kahn J, Kollet O et al. Cycling G1 CD34 /CD38 cells potentiate the motility and engraftment of quiescent G0 CD34 /CD38-/low severe combined immunodeficiency repopulating cells. STEM CELLS 2005;23:561–574.
23 Haylock DN, Williams B, Johnston HM et al. Hemopoietic stem cells with higher hemopoietic potential reside at the bone marrow endosteum. STEM CELLS 2007;25:1062–1069.
24 Arai F, Hirao A, Ohmura M et al. Tie2/angiopoietin-1 signaling regulates hematopoietic stem cell quiescence in the bone marrow niche. Cell 2004;118:149–161.
25 Mazurier F, Doedens M, Gan OI et al. Rapid myeloerythroid repopulation after intrafemoral transplantation of NOD-SCID mice reveals a new class of human stem cells. Nat Med 2003;9:959–963.
26 Cashman J, Dykstra B, Clark-Lewis I et al. Changes in the proliferative activity of human hematopoietic stem cells in NOD/SCID mice and enhancement of their transplantability after in vivo treatment with cell cycle inhibitors. J Exp Med 2002;196:1141–1149.
27 Glimm H, Schmidt M, Fischer M et al. Efficient marking of human cells with rapid but transient repopulating activity in autografted recipients. Blood 2005;106:893–898.
28 Jordan CT, Lemischka IR. Clonal and systemic analysis of long-term hematopoiesis in the mouse. Genes Dev 1990;4:220–232.
29 Abkowitz JL, Persik MT, Shelton GH et al. Behavior of hematopoietic stem cells in a large animal. Proc Natl Acad Sci U S A 1995;92:2031–2035.
30 Laukkanen MO, Kuramoto K, Calmels B et al. Low-dose total body irradiation causes clonal fluctuation of primate hematopoietic stem and progenitor cells. Blood 2005;105:1010–1015.
31 Kuramoto K, Follman D, Hematti P et al. The impact of low-dose busulfan on clonal dynamics in nonhuman primates. Blood 2004;104:1273–1280.
32 McKenzie JL, Gan OI, Doedens M et al. Individual stem cells with highly variable proliferation and self-renewal properties comprise the human hematopoietic stem cell compartment. Nat Immunol 2006;7:1225–1233.
33 Peled A, Petit I, Kollet O et al. Dependence of human stem cell engraftment and repopulation of NOD/SCID mice on CXCR4. Science 1999;283:845–848.
34 Dar A, Kollet O, Lapidot T. Mutual, reciprocal SDF-1/CXCR4 interactions between hematopoietic and bone marrow stromal cells regulate human stem cell migration and development in NOD/SCID chimeric mice. Exp Hematol 2006;34:967–975.
35 Yahata T, Ando K, Sato T et al. A highly sensitive strategy for SCID-repopulating cell assay by direct injection of primitive human hematopoietic cells into NOD/SCID mice bone marrow. Blood 2003;101:2905–2913.
36 Peled A, Kollet O, Ponomaryov T et al. The chemokine SDF-1 activates the integrins LFA-1, VLA-4, and VLA-5 on immature human CD34( ) cells: Role in transendothelial/stromal migration and engraftment of NOD/SCID mice. Blood 2000;95:3289–3296.
37 Prosper F, Stroncek D, McCarthy JB et al. Mobilization and homing of peripheral blood progenitors is related to reversible downregulation of alpha4 beta1 integrin expression and function. J Clin Invest 1998;101:2456–2467.

See www.StemCells.com for supplemental material available online.

Development of Human Graafian Follicles Following Transplantation of Human Ovarian Tissue into NOD/SCID/γcnull Mice

Yukihiro Terada[1], Yumi Terunuma-Sato[1], Tomoko Kakoi-Yoshimoto[1], Hisataka Hasegawa[1], Tomohisa Ugajin[1], Yoshio Koyanagi[2], Mamoru Ito[3], Takashi Murakami[1], Hironobu Sasano[4], Nobuo Yaegashi[1], Kunihiro Okamura[1]

[1]Department of Obstetrics and Gynecology, Tohoku University Graduate School of Medicine, Sendai, Miyagi, Japan;
[2]Viral Pathogenesis Research Center for AIDS, Institute of Viral Research, Kyoto University, Kyoto, Japan;
[3]Central Institute for Experimental Animals, Kawasaki, Japan;
[4]Department of Pathology, Tohoku University Graduate School of Medicine, Sendai, Miyagi, Japan

Keywords
Graafian follicle, human ovarian cortex, NOG mice, ovarian bursa, xenotransplantation

Correspondence
Yukihiro Terada, Department of Obstetrics and Gynecology, Tohoku University School of Medicine, Seryo-machi, Aoba-ku, Sendai, Miyagi 980-8574, Japan.
E-mail: terada@mail.tains.tohoku.ac.jp

Submitted July 8, 2008;
accepted August 25, 2008.

Citation
Terada Y, Terunuma-Sato Y, Kakoi-Yoshimoto T, Hasegawa H, Ugajin T, Koyanagi Y, Ito M, Murakami T, Sasano H, Yaegashi N, Okamura K. Development of human Graafian follicles following transplantation of human ovarian tissue into NOD/SCID/γcnull mice. Am J Reprod Immunol 2008; 60: 534–540

doi:10.1111/j.1600-0897.2008.00653.x

Problem
Transplantation of human ovarian cortex into host mice may permit various kinds of challenges in reproductive medicine. A novel immunodeficient mouse strain (NOD/SCID/γcnull: NOG) has been developed as a host of transplantation of human tissue.

Method of study
Human ovarian cortex was transplanted into various sites of NOG mice and human follicular development was examined by immunohistochemistry.

Results
Transplantation of human ovarian tissue into NOG mice resulted in approximately similar tissue survival and follicle growth as did transplantation into non-obese diabetic-severe combined immunodeficient mice. The human Graafian follicule from NOG mouse expressed the same steroidogenic enzymes as observed in human Graafian follicles, which developed in the human body. The NOG mice's ovarian bursa was better placed for transplantation than the back skin or kidney capsule.

Conclusion
These results represent the successful generation and biological confirmation of the human Graafian follicles from the human ovarian cortex in the NOG mice.

Introduction

Transplantation of human ovarian tissue into immunodeficient mice has been reported to support follicular development of grafted tissue and may provide an alternative means of obtaining human oocytes from ovarian tissue.[1,2] T and B cell-deficient severe combined immunodeficient (SCID) mice and their derivative strains have successfully been used as hosts for transplantation of human tissue, including thymus, bone, and ovary.[3] Among the available strains, the non-obese diabetic (NOD)/SCID strain is generally preferred because of its defects in innate immunity.[3] Antral follicle development has been reported using fresh and cryopreserved human ovarian tissue following transplantation into SCID

American Journal of Reproductive Immunology 60 (2008) 534–540

mice,[4,5] but so far, there has been no evidence that xenografted human ovarian tissue can develop into a mature Graafian follicle. Indeed, the diameter of human antral stage follicles following transplantation into a NOD/SCID mouse ranged between 0.1 and 5.0 mm,[4,6] far short of the 20 mm average diameter of normal, mature human follicles (Graafian follicles), suggesting that their development was arrested at an immature stage. Nonetheless, the possibility that transplantation of frozen-thawed ovarian tissue into an animal host may allow subsequent maturation and collection of matured oocytes offers considerable advantages.

Despite the obvious interest human follicular development and ovulation hold for reproductive medicine, the mechanisms underlying these processes are still poorly understood. As a result, the success rate for assisted reproductive technology remains low. The major reason for this slow progress is the lack of an experimental system in which the development of human primodial follicles into Graafian follicles can be examined.[7,8] Thus, the establishment of a system in which Graafian follicles can develop from human ovarian cortical tissue outside the human body will be useful, not only for the establishment of ovarian banks but also for elucidation of human follicular development.

Several factors may contribute to the observed arrest of follicular development following xenotransplantation. First, although NOD-SCID mice have been reported to be an ideal host, they retain natural killer cell (NK) activity, which can have negative consequences for xenotransplantation.[3] NOD/SCID/γcnull (NOG) mice, which were generated by eight backcross matings of C57BL/6J-/interleukin -2Rγ allelic mutation (γcnull) mice and NOD-SCID mice,[9] possess multiple immunological defects ranging from defects in cytokine production to the functional incompetence of T, B, and NK cells. These features should provide superb conditions for the development of a xenotransplanted graft. Indeed, the success rates for xenografts of human hematopoietic cells[9] and human myeloma cells[10] into host NOG mice are quite promising. Second, the site of transplantation may be an important factor in promoting the maturation of grafted follicles. Although the site of transplantation has been shown to be important for the success of autologous transplantation of human tissue,[11] it is unclear whether or not it affects follicular development of xenografted human ovarian tissue. Transplantation of human ovarian tissue into mice has largely been performed in the back skin, because it is technically easier than transplantation into the kidney capsule or ovarian bursa and allows easy stimulation and monitoring of follicular development.[4] However, it is unknown whether or not other sites of transplantation will permit improved follicular development.

Here, we report the successful generation of human Graafian follicles following transplantation of human ovarian cortex into NOG mice. These follicles possess characteristics of human Graafian follicles, as assessed by the presence of steroidogenic enzymes. We also compared the survival rates and follicular development of ovarian tissue following transplantation into various host tissues in NOG mice and found that the ovarian bursa supports the survival and production of mature Graafian follicles.

Materials and methods

All procedures for collecting human specimens and animal experiments in this study were approved by the Ethics Committee at Tohoku University School of Medicine.

Animals

NOG mice were generated by eight backcross matings of C57BL/6Jγcnull mice and NOD/Shi-scid mice. Female NOG mice and female NOD-SCID mice were maintained in the Central Institute for Experimental Animals (Kawasaki, Japan) and used at 8–10 weeks of age.

Collection of Human Ovarian Cortex

Ovarian cortex tissue was donated following informed, written consent by women undergoing obstetrical/gynecological operations (five caesarean sections, one abdominal myomectomy, all 21–28 years of age). Ovarian tissue was immediately placed in warm phosphate buffered saline medium supplemented with 5 IU/L of follicle stimulating hormone (Fertinome; Serono, ON, Canada) and transported to our facility. Ovarian cortex was cut into small pieces (2 × 2 × 2 mm) and transplanted into immunodeficient mice.

Xenotransplantation and Ovarian Stimulation

The mice were housed in air-filtered isolator cages, and all surgical procedures were performed in the